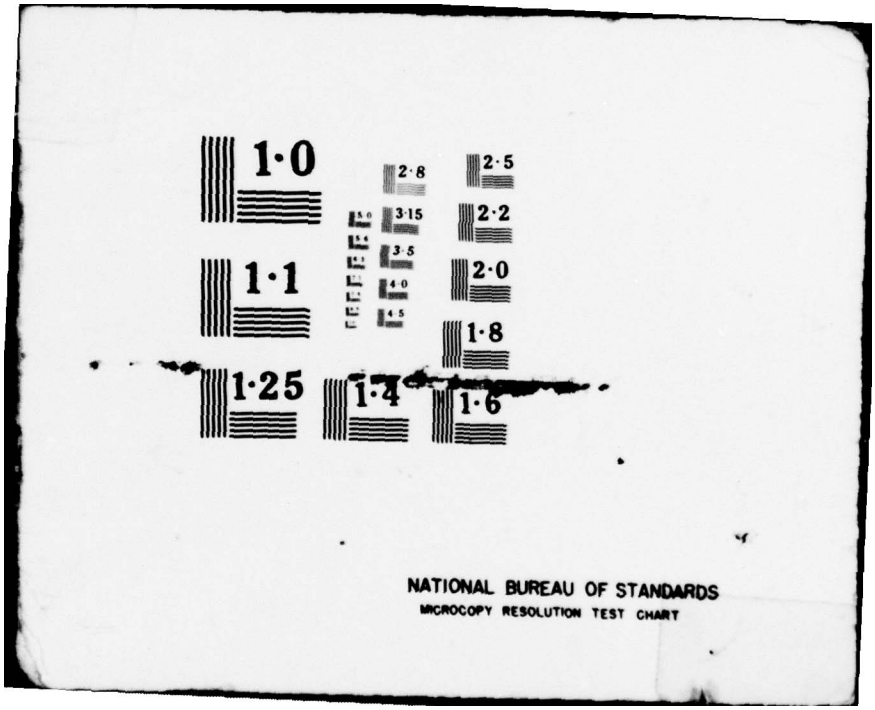
AD-A070 252 SYSTEMS CONTROL INC PALO ALTO CALIF F/G 1/3
PATH CONTROLLERS: UNIFICATION OF CONCEPTS AND COMPARISON OF DES--ETC(U)
DEC 78 J E JONES, J S KARMARKAR F33615-77-C-3079
UNCLASSIFIED AFFDL-TR-78-178 NL

1 OF 2
AD
A070252




1·0
1·1
1·25
1·4
1·6
1·8
2·0
2·2
2·5
2·8
3·15
3·5
4·0
4·5
NATIONAL BUREAU OF STANDARDS
MICROCOPY RESOLUTION TEST CHART

AD A070252

LEVEL II

AFFDL-TR-78-178

PATH CONTROLLERS: UNIFICATION OF CONCEPTS AND COMPARISON OF DESIGN METHODS

J. E. JONES
J. S. KARMARKAR

Systems Control, Inc. (Vt)
1801 Page Mill Road
Palo Alto, CA 94304

DDC RECEIVED JUN 22 1979 C

DECEMBER 1978

DDC FILE COPY

FINAL REPORT: SEPTEMBER 1977 - SEPTEMBER 1978

Approved for public release; distribution unlimited.

AIR FORCE FLIGHT DYNAMICS LABORATORY
AIR FORCE WRIGHT AERONAUTICAL LABORATORIES
AIR FORCE SYSTEMS COMMAND
WRIGHT-PATTERSON AIR FORCE BASE, OHIO 45433

79 06 13 052

NOTICE

When Government drawings, specifications, or other data are used for any purpose other than in connection with a definitely related Government procurement operation, the United States Government thereby incurs no responsibility nor any obligation whatsoever; and the fact that the government may have formulated, furnished, or in any way supplied the said drawings, specifications, or other data, is not to be regarded by implication or otherwise as in any manner licensing the holder or any other person or corporation, or conveying any rights or permission to manufacture, use, or sell any patented invention that may in any way be related thereto.

This report has been reviewed by the Information Office (OI) and is releasable to the National Technical Information Service (NTIS). At NTIS, it will be available to the general public, including foreign nations.

This technical report has been reviewed and is approved for publication.

Jim J. Duckian

JIM J. GUCKIAN, Project Engineer
Control Management Group
Control Systems Development Branch

James W. Morris

JAMES W. MORRIS, Chief
Control Systems Development Branch
Flight Control Division

FOR THE COMMANDER

James R. Stanley

JAMES R. STANLEY, Colonel, USAF
Chief, Flight Control Division

"If your address has changed, if you wish to be removed from our mailing list, or if the addressee is no longer employed by your organization please notify AFFDL/FGL *, W-PAFB, OH 45433 to help us maintain a current mailing list".*

Copies of this report should not be returned unless return is required by security considerations, contractual obligations, or notice on a specific document.

AIR FORCE/56780/13 March 1979 — 50

SECURITY CLASSIFICATION OF THIS PAGE (When Data Entered)

REPORT DOCUMENTATION PAGE

READ INSTRUCTIONS BEFORE COMPLETING FORM

1. REPORT NUMBER: AFFDL-TR-78-178	2. GOVT ACCESSION NO.
3. RECIPIENT'S CATALOG NUMBER	
4. TITLE (and Subtitle): PATH CONTROLLERS: UNIFICATION OF CONCEPTS AND COMPARISON OF DESIGN METHODS.	5. TYPE OF REPORT & PERIOD COVERED: Final Technical Report. September 1977–September 1978
6. PERFORMING ORG. REPORT NUMBER	
7. AUTHOR(s): J.E. Jones, J.S. Karmarkar	8. CONTRACT OR GRANT NUMBER(s): F33615-77-C-3079
9. PERFORMING ORGANIZATION NAME AND ADDRESS: Systems Control, Inc. (Vt), 1801 Page Mill Road, Palo Alto, CA 94304	10. PROGRAM ELEMENT, PROJECT, TASK AREA & WORK UNIT NUMBERS: 62201F, 2403-02-37, 17 02
11. CONTROLLING OFFICE NAME AND ADDRESS: Air Force Flight Dynamics Laboratory(FGL), AF Wright Aeronautical Laboratories, AFSC, Wright-Patterson AFB, Ohio 45433	12. REPORT DATE: December 1978 13. NUMBER OF PAGES: 111
14. MONITORING AGENCY NAME & ADDRESS (if different from Controlling Office): 12 112 3 p.	15. SECURITY CLASS. (of this report): UNCLASSIFIED 15a. DECLASSIFICATION/DOWNGRADING SCHEDULE

16. DISTRIBUTION STATEMENT (of this Report)

Approved for public release; distribution unlimited.

17. DISTRIBUTION STATEMENT (of the abstract entered in Block 20, if different from Report)

18. SUPPLEMENTARY NOTES

19. KEY WORDS (Continue on reverse side if necessary and identify by block number)

Flight Control
Flight Paths
Automatic Control
Control Theory

20. ABSTRACT (Continue on reverse side if necessary and identify by block number)

This report documents the basic theme of a series of seminars presented to the Air Force Flight Dynamics Laboratory concerning the role of modern control theory in advanced aircraft guidance and control concepts. The report discusses a number of optimal guidance and control concepts as cast in a "path-control" formal structure. Trajectory generation concepts include horizontal guidance with and without controlled time of arrival, threat avoidance, performance optimization, and terrain following. Control concepts include linear optimal control and classical techniques. Research areas of high potential payoff are identified.

DD FORM 1 JAN 73 1473 EDITION OF 1 NOV 65 IS OBSOLETE

UNCLASSIFIED

SECURITY CLASSIFICATION OF THIS PAGE (When Data Entered)

389 333

FOREWORD

This report documents the results of efforts conducted under Contract No. F33615-77-C-3079 with the Air Force Flight Dynamics Laboratory, Wright-Patterson Air Force Base. Mr. Jim Guckian was the Project Monitor. This effort was conducted under Project 2403, "Flight Control Technology," Task 240302, "Flight Control Systems Development," Work Unit 2403-02-37, "Flight Control Law Design/Validation."

This investigation was performed during the period from September 1977 to September 1978, and the report was submitted to AFFDL in October 1978.

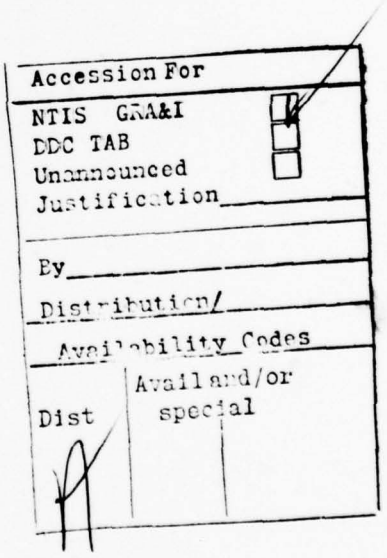


TABLE OF CONTENTS

Section		Page
I	INTRODUCTION	1
	1. Background	1
	2. Scope	6
II	CONTROL SYSTEM DESIGN OVERVIEW	7
	1. Introduction	7
	2. System Modeling	10
	a. Nonlinear System Model	11
	b. Reference Trajectory	13
	c. Linear System Model	14
	d. Reduced Order Modeling	17
	e. Aircraft State Models	26
	3. Design Approaches	27
	a. Nonlinear Optimal Control	28
	b. Linear Optimal Control	37
	c. Comparison to Classical Methods	46
III	PATH CONTROL SYSTEM DESIGN	49
	1. Introduction	49
	2. System Partitioning	50
	3. Reference Generation	52
	a. Horizontal Guidance	54
	b. Vertical Guidance	69
	c. Calculation of Remaining Reference Quantities	79
	4. Perturbation Control	81
	a. Lateral-axis Perturbation Contol Design by Pole Placement Methods	82
	b. STOL Flare Autopilot Design by Quadratic Synthesis	87
IV	CONCLUSIONS AND RECOMMENDATIONS	94
	1. Conclusions	94
	2. Recommended Study Areas	95

TABLE OF CONTENTS (Cont'd)

Section		Page
	a. Threat Avoidance	96
	b. Terrain Following	97
	c. Advanced Perturbation Control	97
APPENDIX		99
REFERENCES		109

LIST OF FIGURES

		Page
1	Illustration of the Path Control Framework of Modern Flight Guidance and Control Systems	2
2	Illustration of the Factors which Influence the Design of Path-Following Systems	2
3	Utilization of Mathematical Models in the Flight Control System Design Process	9
4	Structure of the Mathematical Model of a Physical Process	12
5	Evolution of the State Vector or Trajectory (Example for Three-Dimensional State)	12
6	The Actual and Reference Trajectories, and the Perturbation State $\delta\underline{x}(t)$	15
7	Structure of the Linear (Perturbation) Model of a Physical Process	16
8	Reduction of Model Order by Elimination of Unobservable or Uncontrollable Subsystems	18
9	Illustration of the Singular Perturbation Solution .	21
10	Optimal Open-Loop Control – $\underline{u}_{opt}$ Is Calculated *a priori* and Stored	38
11	Optimal Closed-Loop Control – $\underline{u}_{opt}$ Is Calculated from State Feedback	38
12	Illustration of Minimal On-Line Computational Requirements When Reference State and Reference Control Can Be Pre-Calculated	42
13	Typical Design Activities in the Formulation, Solution and Implementation of the Linear-Quadratic Design	44
14	Comparison of the Basic System Structures of Classical and Optimal Control Theory (Example: Single-Input/Single-Output)	47
15	Generic Block Diagram of a Path Control System . . .	50
16	Definition of Path-Length Reference Parameter L_1 and L_2	60
17	Candidate Profiles for Speed Control Algorithm . . .	60
18	Symbology Used in Threat Avoidance Simulation Examples	63

LIST OF FIGURES (Cont'd.)

		Page
19	Simulation Results Summary for Example Threat Scenario and Minimum Path [28]	65
20	Optimum Flight Path Assuming No Additional Knowledge of Threats Is Gained [28]	66
21	Optimum Flight Path Four Minutes Into the Flight Assuming Uncertainty in Threat C1 Eliminated Due to Onboard Sensors [28]	68
22	Typical Minimum-Time Climb Path to Higher Energy Level [18]	72
23	Comparison of "Exact" and Energy-State Minimum Time-to-Climb Paths [18]	73
24	Comparison of Minimum-Fuel Climbs Using Standard Flight Profile and Approximately Optimal Path at Military Thrust [25]	75
25	Minimum-Fuel Climb, Cruise, Descent – Altitude versus Mach Number	76
26	Minimum-Fuel Climb, Cruise, Descent – Altitude and Fuel versus Range	76
27	Cubic Spline Reference Path [32]	80
28	Energy Constraints Used to Determine V_R	80
29	Moving Target Coordinate System [27].	84
30	Structure of the Perturbation Feedback Control System	86
31	Root Locus of Closed-Loop Feedback Systems [27] . . .	86
32	Typical STOL Flare Maneuver [33]	88
33	Longitudinal Dynamics of Typical STOL Aircraft [33] .	91
34	Altitude vs. Range from Linear Simulation Using Time-Varying Feedback Gain	93
A.1	Forces in the Aircraft Plane of Symmetry	105

LIST OF TABLES

		Page
1	Examples of the Generality of the Performance Index Structural Form	30
2	Illustration of Typical End Conditions and Associated Transversality Expressions	35
3	Survey of Aircraft Performance Optimization Literature	53
4	Terminal and Along-Path Weightings for Flare Autopilot Design	93

LIST OF SYMBOLS

$A(t)$ nxn state matrix $(\partial \underline{f}/\partial \underline{x})$ evaluated along the reference trajectory

$B(t)$ nxm control matrix $(\partial \underline{f}/\partial \underline{u})$

$C(t)$ rxn state measurement matrix $(\partial \underline{g}/\partial \underline{x})$

c_t time weighting factor

c_f fuel weighting factor

$D(t)$ rxm control measurement matrix $(\partial \underline{g}/\partial \underline{u})$

D drag

E energy per unit mass

e elevator deflection

$\underline{f}$ nx1 vector operator which describes the "evolution" (movement) of the state

F flap setting (fixed at the value F_R)

f_ℓ lateral force

g acceleration of gravity

$\underline{g}$ rx1 vector operator which relates the system outputs (measurements) to the states and controls

h altitude

H Hamiltonian

J cost functional or performance index

K mxn linear feedback gain matrix

l penalty functional on state and controls over the controlled interval

m mass

n nozzle deflection (thrust vector)

$Q(t)$ nxn weighting matrix on the along-path state error

q pitch rate

R turn radius

$R(t)$ mxm weighting matrix on the control deviation from nominal

S Ricatti matrix

S_f nxn weighting matrix on the terminal state error

T thrust

T transformation matrix composed of the column eigenvectors of A

t time

$\underline{u}$ mxl vector of controllable variables, or control vector

V velocity

W_h altitude weighting coefficient

W_u control weighting coefficient

$\underline{x}$ nxl vector of dependent variables, or state vector

x,y planar coordinates of position

$\underline{y}$ rxl vector of measurable or output variables

γ flight path angle

$\delta\underline{u}$ variational (perturbation) control vector

$\delta\underline{x}$ variational (perturbation) state vector

Λ nxn block diagonal matrix

λ Lagrange multiplier

Ξ nxm modal control distribution matrix

ν Lagrange multiplier

Φ Mayer functional

ϕ penalty on terminal state

ϕ bank angle

ψ heading angle

SECTION I
INTRODUCTION

1. BACKGROUND

The path control problem, namely, the command and control of an aircraft to follow a reference path, occurs frequently in the design of modern flight guidance and control systems. The problem is two-fold: (1) generating the reference path to satisfy various navigation, guidance or other "outer loop" control objectives such as performance optimization, and (2) following the reference path while simultaneously satisfying "inner-loop" control objectives such as disturbance rejection and insensitivity to vehicle parameter variations.

As will be demonstrated in this report, many aspects of aircraft guidance and control can be (and historically have been) formulated in this path control framework, which is illustrated in Figure 1. Referring to the figure, the path control framework consists of two parts: (1) a "reference generator" which defines reference trajectories and nominal control commands that satisfy outer-loop control objectives, and (2) a "perturbation controller" which effects a perturbation control that satisfies inner-loop control objectives. The nominal control and perturbation control are then summed to yield the total control command which is sent to the control actuators.

Several factors work together to heighten the importance of the path control problem and to diversify the ways in which it appears. As illustrated in Figure 2, changing Air Force mission requirements and the advent of Control Configured Vehicle (CCV) technology have had a profound influence on the requirements for both outer loop and inner loop control design. At the same time, advances in the capabilities for on-board processing have

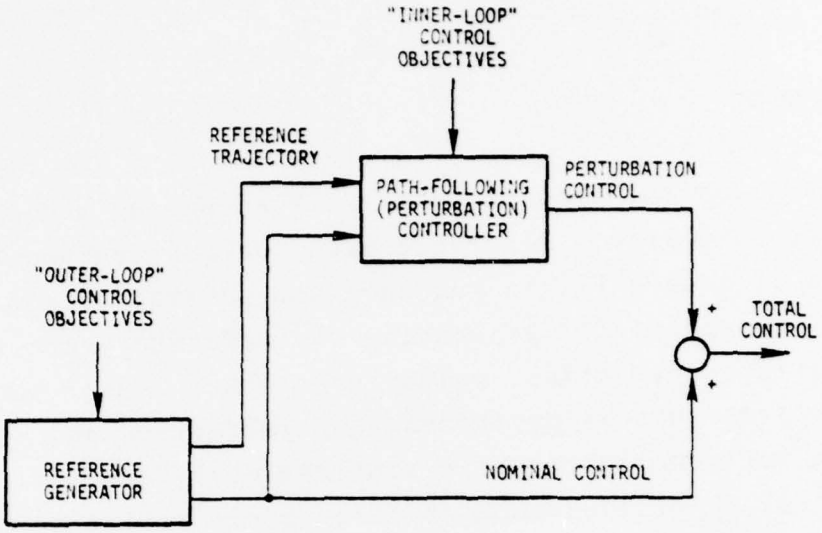


Figure 1. Illustration of the Path Control Framework of Modern Flight Guidance and Control Systems

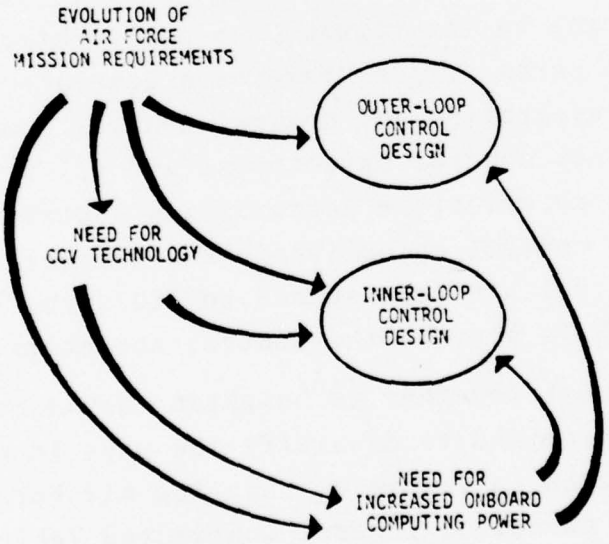


Figure 2. Illustration of the Factors which Influence the Design of Path-Following Systems

improved the "implementability" of sophisticated designs. The interrelationship of these factors is discussed below.

Air Force mission requirements have evolved to encompass the flying of complex trajectories to improve the effectiveness and safety of tactical operations, such as rendezvous for refueling or aerial delivery (time-of-arrival guidance) and minimizing exposure to the enemy (terrain following, threat avoidance). Synthesis of the required complex trajectories can, in many cases, be viewed directly as the reference generation portion of the path control problem. Further, the Air Force, as well as civil aviation, is increasingly aware of energy efficiency. Consequently, much effort has been directed towards fuel-economic operations. In the context of "outer loop" control, several techniques have been applied to generate reference paths which optimize fuel consumption by managing the aircraft's energy state. Fuel optimization can also be addressed at the inner control loop. For example, the presence of direct lift control provides an additional, redundant means of regulating aircraft pitch-plane motion; consequently, a path-following controller for this application may well be designed to follow its reference while simultaneously attempting to optimize the thrust control level.

Direct lift control and other automated techniques which aim at augmenting the basic stability, handling qualities, and performance characteristics of aircraft fall into the general category of CCV technology. The key idea of CCV technology is the integration of control with aerodynamics, structures, and propulsion early in the design cycle of the aircraft. Studies have shown that significant reductions in induced drag and structural weight and reduction of flight hazards can be achieved with such active controls [1]. These benefits are possible due to (1) a reduction in the sizes of stabilizing surfaces, with stability provided by dynamically controlling movable

surfaces rather than statically with large fixed surfaces as in the conventional designs; (2) reductions in structural strength requirements (and hence weight) by applying maneuver load alleviation and gust load alleviation; and (3) reduction in the occurrence of inadvertent flight hazard through automatic limitation of flight conditions. Many of the objectives of these active controls can be expressed as additional performance criteria and design constraints for the path-following portion ("inner loop") of the path control system.

A very important example of how Air Force mission requirements and CCV technology relate to the path control problem is the recent work [2,3] aimed at providing aircraft (YC-14, YC-15, and various NASA research aircraft) capable of short take-off and landing (STOL). The STOL investigations are developing powered-lift technology, exploring such concepts as the augmentor wing, lift fan, and externally blown flap. These concepts all achieve the necessary wide range of lift coefficient by means of in-flight modifications to the aircraft configuration. Such modifications result in extreme changes in the control characteristics of the aircraft in the transition from cruising flight to the high-lift landing configuration.

For the STOL problem, the path generation function must satisfy the typically more stringent short-field landing performance requirements, in terms of minimum dispersions in the vicinity of the touchdown point. Synthesis of the reference path must also contend with the changes in aircraft characteristics associated with transitions in the aircraft configuration. The design of the inner loop (or path-following or "perturbation") controller is also affected by these transitions in that the aircraft response to controls over the full flight envelope is very nonlinear. Moreover, the presence of powered- and direct-lift generators increases the total number of

controls available to the pilot* who must continually make decisions on control techniques. Accurate, unaided, manual tracking of complex trajectories by manipulating a large set of interacting controls of an aircraft whose control characteristics are nonlinear and rapidly changing represents an unacceptably high pilot workload [1]. Thus, the path-following portion of the control system is tasked with automatic resolution of ambiguous controls and the maintenance of acceptable and consistent handling qualities, in addition to stringent tracking of its input commands.

Of course, the scale of CCV technology would have been severely restrained had it not been for the rapidly advancing technology of electronics and especially airborne computing. Modern flight control systems are capable of substantial reliability requirements associated with active controls, many of which are critical to flight safety. Computation resource is vital to implementational feasibility of path control systems. The generation of reference paths, for example, typically requires the solution of an optimization problem (minimum fuel, minimum time, etc.) over a wide range of flight conditions and subject to numerous constraints. Such a reference solution can be very resource consuming, depending strongly on the problem addressed and the numerical methods used. Fortunately, the dynamics of the outer (reference) solution are, in general, relatively slow; consequently, a reduced iteration interval can usually be employed for the reference solution, thus spreading the processing over a number of basic computational cycles. Such implementational considerations will be discussed in this report as appropriate in the context of path control.

* Typically, the pilot will intervene to provide the outer-loop/inner-loop interface for such sensitive STOL operations as the transition, landing, and take-off phases.

2. SCOPE

The preceding discussion has pointed out the diversity of control objectives which impact the design of modern flight control systems. To meet these objectives, there has been a proliferation of analytic methods and design approaches, exhibiting varying degrees of success and practicality. Some problem areas have received a great deal of attention; others have received very little.

The purpose of this report is to unify design concepts for modern flight guidance/control systems, to compare design methods as to their applicability and promise, and to identify areas toward which future research should be directed. In order to provide a basis for the unification of concepts, the report casts a number of typical aircraft mission requirements and control design objectives in the framework of the path control problem. In this context, design methods are reviewed for both reference (trajectory) generation and path-following (perturbation) control, and a number of illustrative examples are presented. The report does not include rigorous derivations of the design methods; rather, the emphasis is on the basic principles behind the methods and their applicability to the various facets of the path control problem. Where appropriate, computational requirements and design constraints are also discussed.

The remainder of this report is organized as follows. Section II presents an overview of control system design objectives, constraints, and methods. The role of system modeling in the design process is discussed, and a fairly comprehensive development of system modeling techniques is presented. Section III defines the path control generic structure and identifies ways in which broad design problems are decomposed and partitioned to conform to this framework. The reference generation and perturbation (path-following) portions of the path control problem are then discussed separately. Section IV presents conclusions and recommendations for future work.

SECTION II
CONTROL SYSTEM DESIGN OVERVIEW

1. INTRODUCTION

Control of modern, complex flight systems is a broad and multifaceted problem. The flight control system must provide for safe and efficient accomplishment of the control objectives. At the highest level, these control objectives might be described as any one or combination of the following, among others:

- Control of along-path or terminal errors
- Economic control of time, fuel, or energy expenditure
- Achieving or maintaining a desired separation distance (e.g. in-flight refueling)
- Achieving a desired terminal state (altitude, velocity, etc.)
- Avoiding hazardous obstacles, terrain, or threat contours

At the middle and lower levels, control objectives address such related issues as:

- Augmentation of the basic stability characteristics of the aircraft
- Enhancement of the aircraft's flying qualities
- Alleviation of structural loads
- Limiting the flight envelope to exclude hazardous flight conditions

In meeting the varied and sometimes conflicting control objectives, the flight control system must deal with many constraints and limitations. Among these are:

- Computational constraints (speed and memory sizing) for computerized control algorithms

- Practical limitation of size of aerodynamic surfaces and the effectiveness of associated actuators
- Practical limitation of the number, type, and placement of motion sensors
- Performance constraints of the man/vehicle system

Many methods have been applied to the design of systems to meet the above-mentioned aircraft control objectives in the face of the indicated constraints and limitations. These can be loosely categorized as classical and modern techniques. Classical techniques are normally associated with single-input/single-output transfer functions and design in the frequency domain; modern techniques are characterized by design in the time domain (state-space system description) and the optimization of a multifaceted performance criterion. Although certainly not mutually exclusive, classical techniques have historically been applied to the middle and lower level (inner loop) control objectives cited above; the higher level (outer loop) objectives have normally been addressed by modern optimization techniques. These various design methods are described in more detail in subsequent sections.

Common ground for both classical and modern design methods is their reliance on a mathematical model of the aircraft and its environment. Such a model plays a central role in the design of flight control systems, as illustrated in Figure 3. As shown, the model is used not only for design of the control system itself, but also to aid in the evalution of the resulting design. The model serves as the basis for off-line simulation of the controlled process and evaluation of the flight control system in this simulated environment. The simulation includes, in addition to the control algorithms themselves, detailed models of the significant aircraft systems and environmental conditions. Such simulator models are typically of a higher

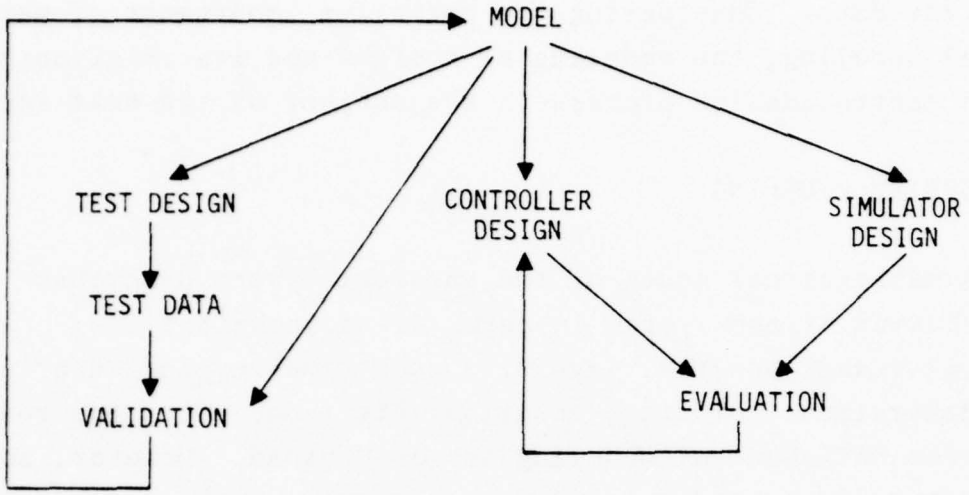


Figure 3. Utilization of Mathematical Models in the Flight Control System Design Process

degree of fidelity (or completeness) than those more simplified* versions which are normally used for control design. The simulation may well include pieces of the actual flight hardware subsystems in place of certain mathematical submodels; in some cases, a complete cockpit mockup is included. As also illustrated in Figure 3, the model is used additionally to plan and direct experimental test and validation activities. Exercising the model in a simulated environment can indicate sensitive aspects of the controller/vehicle system design, so that test activities can be directed towards these sensitive areas. Analysis of the test data has the dual purpose of evaluating the performance of the control system design and also

* Such simplifications to a sophisticated model may be necessary in order to achieve a practically implementable solution.

validating the models upon which the design is based, for example, by statistical identification of the model's parameters from test data. Considering the pervasive importance of mathematical modeling, the modeling of systems and its relationship to the control design process is the subject of the next section.

2. SYSTEM MODELING

A mathematical model of the physical system describes the behavior of the system in terms of mathematical laws of physics and geometry, involving such time-varying quantities as acceleration, velocity, position, attitude, etc. The realm of system mathematical modeling is quite broad. However, for aircraft guidance and control design purposes, the scope can almost always be narrowed to finite-dimensional systems, which means that the system under consideration can be described by a finite number of time-varying quantities (variables). Moreover, the systems to be addressed are of the lumped, continuous time type, which means that they can be modeled in terms of ordinary differential equations.*

The differential equations which represent aircraft motion are well known [4], having their basis in Newton's laws (force equilibrium) and the Euler equations. Further principles of Newtonian mechanics are used to generate equations which relate to the energy state of the aircraft. In some cases, empirical methods may be required to establish certain functional relationships or to quantify parameters in the equations which constitute the mathematical model.

* The basic concepts developed here apply also to discrete time systems, such as systems with measurements at discrete times and/or with control changes at discrete times, and to distributed systems, such as systems with elastic components.

a. Nonlinear System Model

Once established from the laws of physics and geometry, the generally nonlinear equations of motion can be written in the state-space form using vector notation:

$$\dot{\underline{x}} = \underline{f}(\underline{x},\underline{u},t) \tag{1}$$

and

$$\underline{y} = \underline{g}(\underline{x},\underline{u},t) \tag{2}$$

where

$\underline{x}$ is the nx1 vector of dependent variables, or state vector

$\underline{f}$ is an nx1 vector operator which describes the "evolution" (movement) of the state

$\underline{u}$ is the mx1 vector of controllable variables, or control vector

$\underline{y}$ is the rx1 vector of measurable or output variables

$\underline{g}$ is the rx1 vector operator which relates the system outputs (measurements) to the states and controls

t is the time, the independent variable

Equation (1) is called the "state" (or "evolution") equation; Eq. (2) is called the "measurement" (or "output") equation. The mathematical model of the physical process is illustrated in Figure 4. The tip of the state vector describes the state "trajectory," as illustrated in Figure 5. Physical requirements usually yield a continuous trajectory, even though the control $\underline{u}(t)$ may be discontinuous or occur at discrete instants, as in the case of a digitally controlled process.

For modeling aircraft dynamics, the state equation is so formulated as to encompass all significant aerodynamic modes [4].

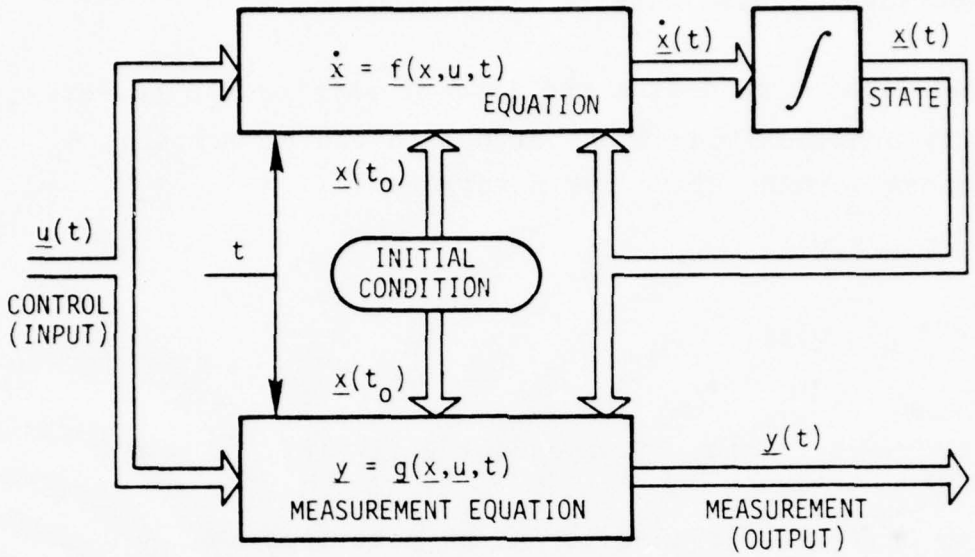


Figure 4. Structure of the Mathematical Model of a Physical Process

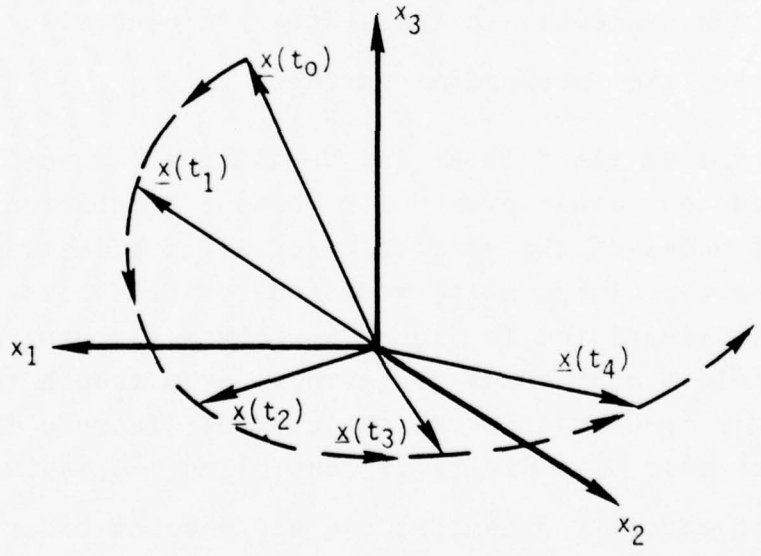


Figure 5. Evolution of the State Vector or Trajectory (Example for Three-Dimensional State)

In addition, actuator and sensor dynamics, if significant, can be absorbed into the state equation.

b. Reference Trajectory

Having arrived at the best available system model (Eqs. (1), (2)), the next logical step is to determine the ideal (or nominal) control $\underline{u}_o(t)$ which will induce the desired ideal (or nominal) behavior of the system state $\underline{x}_o(t)$. Formally, the reference (or nominal) trajectory is described by:

$$\dot{\underline{x}}_o(t) = \underline{f}(\underline{x}_o(t), \underline{u}_o(t), t) \tag{3}$$

$$\underline{y}_o(t) = \underline{g}(\underline{x}_o(t), \underline{u}_o(t), t) \tag{4}$$

The reference trajectory and control may be obtained in a number of ways, ranging from various ad hoc methods (trial-and-error computer runs, geometric fitting of curves through "way-points," etc.) to sophisticated optimization procedures (calculus of variations, numerical iterative techniques such as gradient methods or differential dynamic programming, etc.). Section III provides some examples of reference generation for aircraft guidance and control problems.

Unfortunately, the ideal reference control, when input into the real physical system, will not, in general, exactly produce the ideal trajectory; i.e. setting the real control $\underline{u}(t)$ equal to the calculated ideal $\underline{u}_o(t)$ will not yield a true state trajectory $\underline{x}(t)$ which is identically equal to the ideal $\underline{x}_o(t)$ for all t in the interval of interest. The reason is that $x_o(t)$ and $y_o(t)$ were computed using a mathematical model of the physical process. However, the engineer has to make some approximations (sometimes intentionally) to arrive at the mathematical model, often neglecting to include second-order effects. Even if the equations were exact structurally,

the values of the parameters used in the mathematical model are nominal ones and the true values may be slightly different. In addition, the actual initial state of the system $\underline{x}(t_o)$ may differ slightly from the ideally assumed one $\underline{x}_o(t_o)$. It then follows that errors in the deterministic model may by themselves contribute to deviations of the true physical plant state $\underline{x}(t)$ from its ideal deterministic one $\underline{x}_o(t)$. In fact, small initial deviations, caused by the difference $\underline{x}(t_o) - \underline{x}_o(t_o)$, may get worse and worse as time goes on [5]. In order to deal with these deviations, one looks at the behavior of the model in the "neighborhood" of the reference trajectory.

c. Linear System Model

The behavior of the model in the neighborhood of the reference trajectory is described by linear "perturbation equations." If the reference trajectory is truly optimal, then the perturbation equations contain information as to how the model could best be driven back to the original trajectory (for example) after having been perturbed away from the reference trajectory. The perturbation concept, illustrated in Figure 6, is evident in the following definitions:

$\delta\underline{x}(t) \equiv \underline{x}(t) - \underline{x}_o(t)$: perturbation state vector

$\delta\underline{y}(t) \equiv \underline{y}(t) - \underline{y}_o(t)$: perturbation measurement vector

$\delta\underline{u}(t) = \underline{u}(t) - \underline{u}_o(t)$: perturbation control vector

The linear system model emanates from the perturbation concept by expanding the state and measurement equations

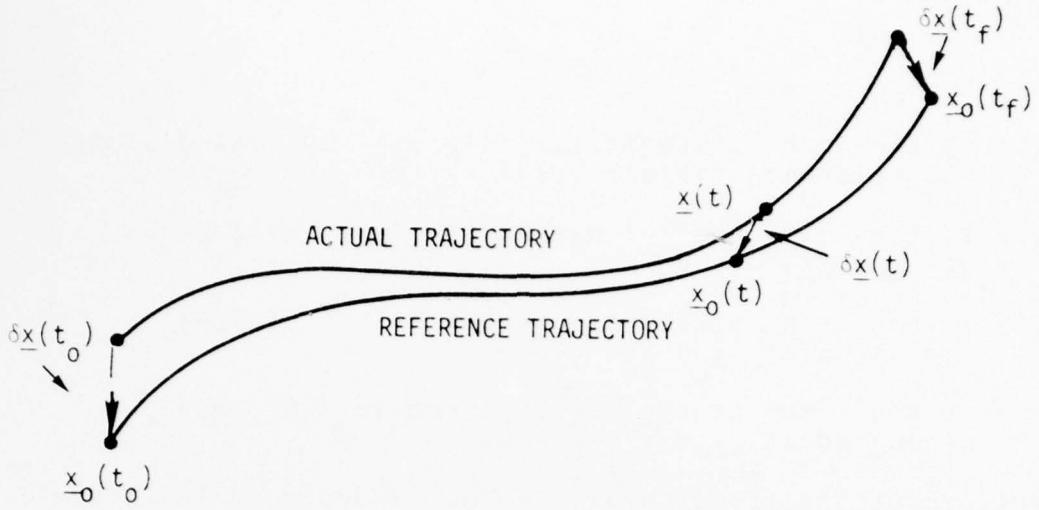


Figure 6. The Actual and Reference Trajectories, and the Perturbation State $\delta\underline{x}(t)$

about the reference values ($\underline{x}_o(t)$ and $\underline{u}_o(t)$) in a Taylor Series:

$$\underline{f}(\underline{x}(t),\underline{u}(t)) = f(\underline{x}_o(t),\underline{u}_o(t)) + \left.\frac{\partial \underline{f}}{\partial \underline{x}}\right|_o \delta\underline{x}(t) + \left.\frac{\partial \underline{f}}{\partial \underline{u}}\right|_o \delta\underline{u}(t) + \underline{\alpha}_o(\delta\underline{x}(t),\delta\underline{u}(t)) \quad (5)$$

$$\underline{g}(\underline{x}(t),\underline{u}(t)) = \underline{g}(\underline{x}_o(t),\underline{u}_o(t)) + \left.\frac{\partial \underline{g}}{\partial \underline{x}}\right|_o \delta\underline{x}(t) + \left.\frac{\partial \underline{g}}{\partial \underline{u}}\right|_o \delta\underline{u}(t) + \underline{\beta}_o(\delta\underline{x}(t),\delta\underline{u}(t)) \quad (6)$$

where the vector functions $\underline{\alpha}_o$ and $\underline{\beta}_o$ represent the higher order terms in the series expansion. If the nominal is subtracted from the above equations and the higher order terms $\underline{\alpha}_o$ and $\underline{\beta}_o$ are neglected, the linear system model results:

$$\delta\dot{\underline{x}}(t) = A(t)\delta\underline{x}(t) + B(t)\delta\underline{u}(t) \quad (7)$$

$$\delta\underline{y}(t) = C(t)\delta\underline{x}(t) + D(t)\delta\underline{u}(t) \quad (8)$$

where

A(t) is the nxn state matrix $(\partial \underline{f}/\partial \underline{x})$ evaluated along the reference trajectory at $\underline{x}_o(t)$ and $\underline{u}_o(t)$

B(t) is the nxm control matrix $(\partial \underline{f}/\partial \underline{u})$ evaluated at $\underline{x} = \underline{x}_o$, $\underline{u} = \underline{u}_o$

C(t) is the rxn state measurement matrix $(\partial \underline{g}/\partial \underline{x})$ evaluated at $\underline{x} = \underline{x}_o$, $\underline{u} = \underline{u}_o$

D(t) is the rxm control measurement matrix $(\partial \underline{g}/\partial \underline{u})$ evaluated at $\underline{x} = \underline{x}_o$, $\underline{u} = \underline{u}_o$

The structure of the linear system model is depicted in Figure 7.

In general, the matrices of partial derivatives A, B, C, and D must be calculated along the reference trajectory; i.e. the elements of the matrices are functions of the reference state and reference control. The system is thus time varying (or nonautonomous). For certain classes of systems, it may be permissible to assume these matrices to be constant over the region and time interval of interest. In this case, the system is classified as time invariant, and the coefficients of the

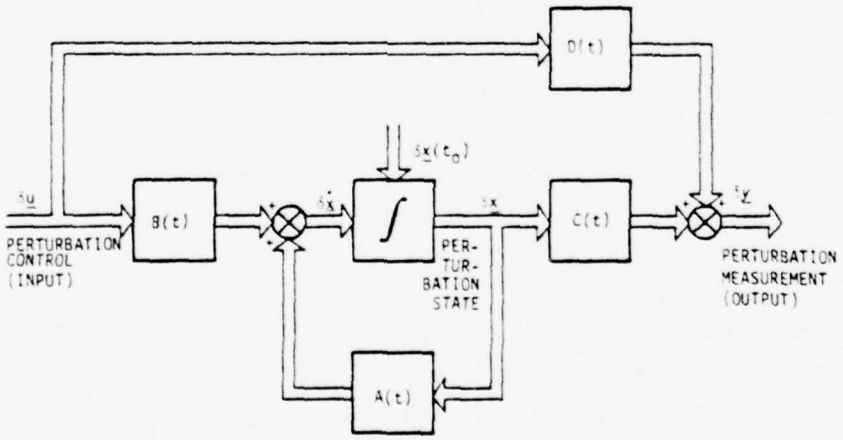


Figure 7. Structure of the Linear (Perturbation) Model of a Physical Process

linear differential equations represented by Eqs. (7) and (8) become constant. The constant coefficient differential equations are amenable to the transform methods which are critical to classical design approaches.

d. Reduced Order Modeling

For the purpose of simply predicting or "simulating" state trajectories, state models of high dimensionality ($n \sim 30$ or more) are well within the computational capabilities of modern large-scale computing systems. However, as a rule, control system design methods, both classical and modern, rapidly become unwieldy as system dimension increases. For this reason, much attention has been given to the reduction of model order. It should be noted that controllers designed using a reduced-order model will be suboptimal. The performance of such suboptimal controllers must be evaluated, generally, in a high-fidelity simulation to determine whether the reduced-order designs are acceptable.

The following outlines some of the more successful methods of reduced-order modeling. Specific examples will be given in subsequent sections.

(1) Neglecting Subsystems

The most basic form of model order reduction is simply ignoring certain subsystems whose states are either not observable or not controllable. An example of this is the neglecting of bending modes whose natural frequencies are beyond the control bandwidth of the actuator which moves a particular aerodynamic surface.

An observable subsystem is one whose initial state $\underline{x}(t_o)$ can be completely and uniquely reconstructed from all subsequent measurements $\underline{y}(t)$ and controls $\underline{u}(t)$ in the interval $[t_o, t_f]$. Similarly, a controllable subsystem is one which can be brought from an arbitrary initial state $\underline{x}(t_o)$ and initial time to a specified terminal state $\underline{x}(t_f)$ within the time span $(t_f - t_o)$. There exist in the literature [6] certain mathematical expressions which test for observability and controllability, notably for linear systems. While these expressions will not be reiterated here, Figure 8 presents an illustration of this most basic concept of model reduction.

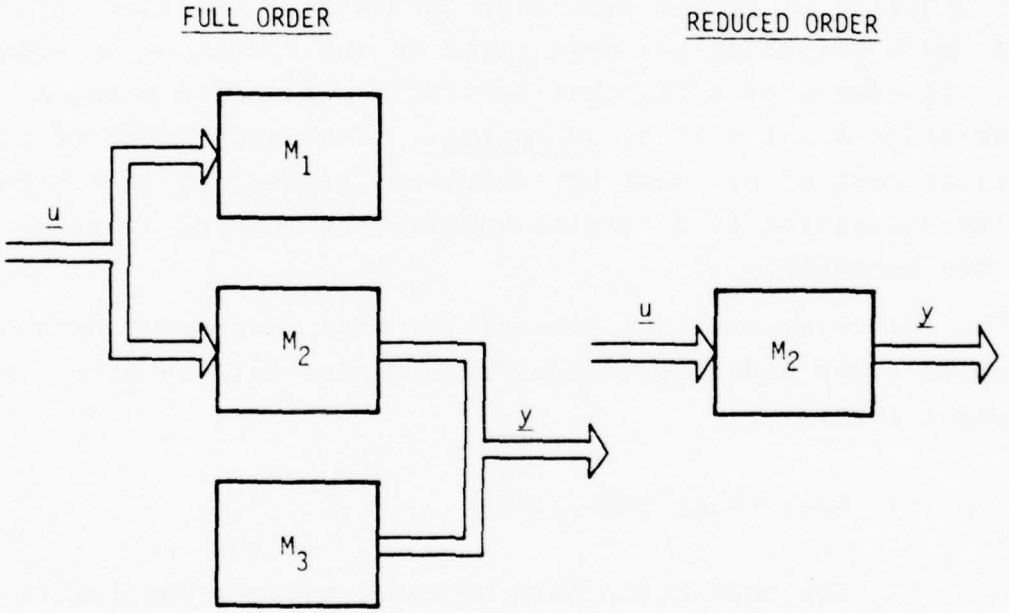


Figure 8. Reduction of Model Order by Elimination of Unobservable or Uncontrollable Subsystems

(2) Singular Perturbations

Neglecting subsystems and system states which are assumed to be insignificant to the control objectives being addressed frequently takes on ad hoc connotations, relying on the experience and engineering judgment of the designer to effect a suitable reduced-order model. A more systematic way of reducing the order of a large class of nonlinear systems, namely, those which exhibit a wide dynamic range (i.e. "slow" and "fast") of characteristic modes, is provided by singular perturbation theory.

Simplistically, the singular perturbation method can be looked upon as a time scaling procedure, which decouples the problem into several problems of a lower order and addresses each of these at an appropriate time scale. The method first defines the slowest time scale (or "free-stream" or "outer expansion") dynamics by assuming that all the faster dynamics are in equilibrium. Once this outer solution is determined, the method then investigates the faster time scale (or "boundary layer" or "inner expansion") problem as a correction about this outer solution [7].

The method begins by grouping the states of the high-order model according to a small parameter ε . This small parameter may either occur naturally in the model (such as a short time constant) or it may be introduced intentionally as an artificial time-scaling parameter. The nonlinear state model (Eq. (1)) is then partitioned into the form:

$$\dot{\underline{x}}_1 = \underline{f}_1 (\underline{x}_1, \underline{x}_2, \underline{u}, t) \qquad (9)$$

$$\varepsilon\dot{\underline{x}}_2 = \underline{f}_2 (\underline{x}_1, \underline{x}_2, \underline{u}, t) \qquad (10)$$

where the subscripts 1 and 2 refer to the states associated with the slower and faster dynamics respectively. The method then

seeks a series solution in ε about $\varepsilon=0$; thus ε is set equal to zero in Eq. (10) which reduces to an algebraic relation:

$$0 = \underline{f}_2 (\underline{x}_1, \underline{x}_2, \underline{u}, t) \tag{11}$$

This is equivalent to the faster states $\underline{x}_2$ being in equilibrium. Equation (11) serves as a condition which can be used to eliminate certain of the faster states $\underline{x}_2$ or certain control variables* $\underline{u}$ from Eq. (9). For example, Eq. (11) can be solved for $\underline{x}_2$:

$$\underline{x}_2 = \underline{\phi} (\underline{x}_1, \underline{u}, t) \tag{12}$$

and Eq. (9) is reduced to the order of the slower states $\underline{x}_1$:

$$\dot{\underline{x}}_1 = \underline{f}_1(\underline{x}_1, \underline{\phi}(\underline{x}_1, \underline{u}, \underline{t}), \underline{u}, \underline{t}) = \underline{f}_1'(\underline{x}_1, \underline{u}, \underline{t}) \tag{13}$$

The solution of the outer expansion (Eq. (13)) neglects the dynamics of $\underline{x}_2$; the outer solution will typically have discontinuities (most noticeably at the initial time) because of this assumption that the states $\underline{x}_2$ can change their values instantaneously. The boundary layer (or inner expansion) analysis examines fast phenomena in terms of the parameter ε and provides a correction to the outer solution, as illustrated in Figure 9.

---

* If the outer expansion is to be solved by optimization methods, there are cases where it is mathematically advantageous to eliminate some of the elements of $\underline{u}$ and retain the same number of elements of $\underline{x}_2$ to act as new control variables in the outer solution. For example, pitch angle is a "fast" state in the longitudinal aircraft dynamics, relative to flight path angle, and elevator angle may be the true control variable; the "outer solution" may well be expressed with pitch angle (the equilibrated state), rather than elevator, as an effective control variable. This procedure is particularly effective when the elements of $\underline{u}$ being eliminated appear linearly in the differential equations or cost functional (singular variational problems) or when the elements of $\underline{x}_2$ being retained as new control variables are constrained independently of $\underline{u}$ (state-constrained variational problems) [8].

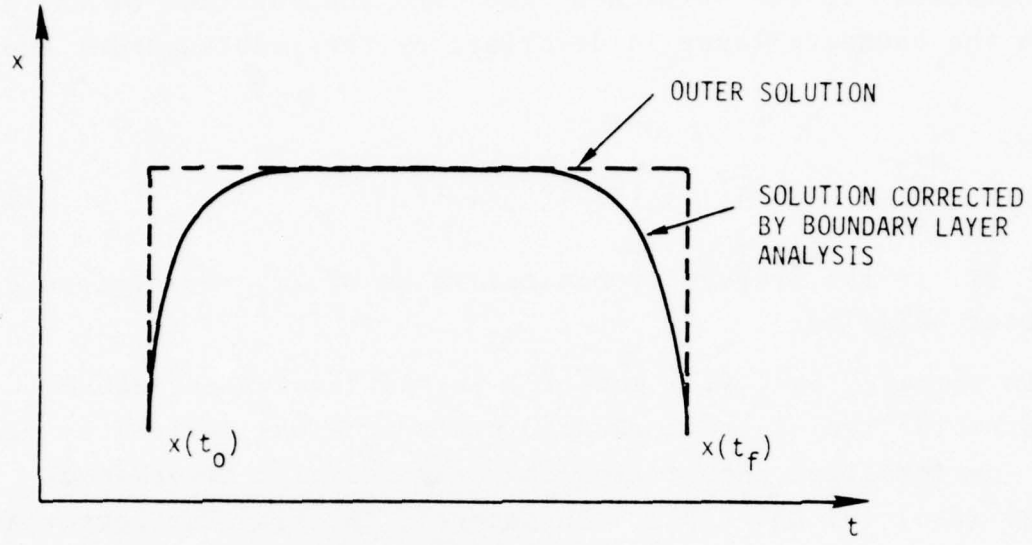


Figure 9. Illustration of the Singular Perturbation Solution

The boundary layer (inner-expansion) is examined by making the time transformation

$$\tau = t/\varepsilon \tag{14}$$

In the "stretched" time scale τ, the original Eqs. (9) and (10) take the form:

$$\frac{d\underline{x}_1}{d\tau} = \varepsilon\, \underline{f}_1(\underline{x}_1, \underline{x}_2, \underline{u}, \varepsilon\tau) \tag{15}$$

$$\frac{d\underline{x}_2}{d\tau} = \underline{f}_2(\underline{x}_1, \underline{x}_2, \underline{u}, \varepsilon\tau) \tag{16}$$

Again letting ε approach zero, the slow variable $\underline{x}_1(\tau)$ appears as a constant* in the stretched time, and the behavior of the system in the boundary layer is described by the reduced-order equation:

$$\frac{d\underline{x}_2}{d\tau} = \underline{f}_2(\bar{\underline{x}}_1, \underline{x}_2(\tau), \underline{u}(\tau), t) \qquad (17)$$

where $\bar{\underline{x}}_1$ is the average or nominal value of $\underline{x}_1$ as defined by the outer solution.

In summary, Eqs. (13) and (17) in the development above represent the two separate reduced-order problems derived by singular perturbation theory from the original high-dimensional problem (Eqs. (9) and (10)). In general, the singular perturbation approach is approximate and the resulting design must be checked for validity. For the case of linear systems, a number of mathematical conditions and techniques have been formulated to "prove" validity of the method under restricted conditions [7]. The singular perturbation methods as applied to aircraft guidance problems is discussed further in Section III.

(3) Modal Decomposition

For the case of linear time-invariant systems in particular, a number of systematic methods have been developed which aim at decomposing the high-order system by identifying its normal modes and then retaining only those which are "dominant" in the system response, i.e., those which are in the frequency range of interest. Such approaches are termed "dominant mode," "dominant eigenvalue," or "pole removal" methods [9, 10].

---

* i.e., Eq. (15) reduces to $d\underline{x}_1/d\tau = 0$.

Basically, these methods proceed as follows. From the previous development, the linear, time-invariant system model can be written:

$$\dot{\delta \underline{x}} = A\ \delta \underline{x} + B\ \delta \underline{u} \tag{18}$$

$$\delta \underline{y} = C\ \delta \underline{x} + D\ \delta \underline{u} \tag{19}$$

This system of equations can be transformed to a canonical (block diagonal) form by the transformation T, which is an nxn matrix composed of the column eigenvectors of A:

$$\delta \underline{x} = T\ \delta \underline{x}' \tag{20}$$

$$\dot{\delta \underline{x}}' = \Lambda\ \delta \underline{x}' + \Xi\ \delta \underline{u} \tag{21}$$

$$\delta \underline{y} = CT\ \delta \underline{x}' + D\ \delta \underline{u} \tag{22}$$

where

Λ is an nxn block diagonal matrix

$\delta \underline{x}'$ is an nx1 vector of modal coordinates

Ξ is an nxm modal control distribution matrix

Once in this form, the characteristic modes of the original system can be examined directly through the block diagonal elements of Λ. One can now partition Λ such that, for example, all "slow" or "dominant" modes are grouped with partition Λ_1 and all "fast" or "removable" modes are grouped with partition Λ_2. The partitioned problem is then:

$$\begin{bmatrix} \delta \underline{x}_1 \\ \hline \delta \underline{x}_2 \end{bmatrix} = \left[\begin{array}{c|c} T_{11} & T_{12} \\ \hline T_{21} & T_{22} \end{array}\right] \begin{bmatrix} \delta \underline{x}_1' \\ \hline \delta \underline{x}_2' \end{bmatrix} \tag{23}$$

$$\begin{bmatrix} \delta\dot{\underline{x}}_1' \\ --- \\ \delta\dot{\underline{x}}_2' \end{bmatrix} = \left[\begin{array}{c|c} \Lambda_1 & 0 \\ \hline 0 & \Lambda_2 \end{array}\right] \begin{bmatrix} \delta\underline{x}_1' \\ --- \\ \delta\underline{x}_2' \end{bmatrix} + \begin{bmatrix} \Xi_1 \\ --- \\ \Xi_2 \end{bmatrix} \delta\underline{u} \tag{24}$$

where $\delta\underline{x}_1$ is of dimension qx1 and $\delta\underline{x}_2$ is of dimension (n-q)x1.

Now if the "fast" modes are assumed to be in equilibrium, then the following reduction can be made: the states $\delta\underline{x}_2'$ are assumed to be equilibrated (i.e., $\delta\dot{\underline{x}}_2' = 0$) and Eq. (24) reduces to a q^{th} order differential equation in $\delta\underline{x}_1'$ and (n-q) algebraic equations in $\delta\underline{x}_2'$. Thus, one can write:

$$\delta\dot{\underline{x}}_1 = A_r\, \delta\underline{x}_1 + B_r\, \delta\underline{u} \tag{25}$$

$$\begin{bmatrix} \delta\underline{x}_2 \\ \delta\underline{y} \end{bmatrix} = \begin{bmatrix} C^* \\ C_r \end{bmatrix} \delta\underline{x}_1 + \begin{bmatrix} D^* \\ D_r \end{bmatrix} \delta\underline{u} \tag{26}$$

where the reduced-model matrices are calculated as:

$$A_r = T_{11}\Lambda_1\, T_{11}^{-1} \tag{27}$$

$$B_r = T_{11}(\Lambda_1 T_{11}^{-1} T_{12} \Lambda_2^{-1} \Xi_2 + \Xi_1) \tag{28}$$

$$C^* = T_{21} T_{11}^{-1} \tag{29}$$

$$D^* = (T_{21} T_{11}^{-1} T_{12} - T_{22}) \Lambda_2^{-1} \Xi_2 \tag{30}$$

$$C_r = C_1 + C_2 C^* \tag{31}$$

$$D_r = D + C_2 D^* \tag{32}$$

Equation (25) is now the q^{th}-order reduced model; the states $\delta\underline{x}_2$ now are observed merely as additional outputs of the

system (Eq. (26)) rather than as dynamic entities. The poles associated with Λ_2 have essentially been "removed" from the problem and only the "dominant" modes Λ_1 are retained.

(4) Control-Sensitive Methods

The previously discussed methods have based their order reduction decisions on the open-loop model; they ignore the specific effects of the control inputs because these inputs are not known a priori. Controllers designed based on the open-loop methods (singular perturbations, dominant eigenvalues, etc.) behave as predicted if the control bandwidth is sufficiently low as to not alter the original "slow" and "fast" designation of the modes. However, if the control objectives require a high bandwidth, those modes originally designated as slow may become fast in closed-loop operation, and performance may deteriorate from that predicted.

Considerable recent effort [11, 12] has been directed towards developing model reduction methods which are "sensitive" to the control objectives. These methods, then, proceed to derive the reduced-order model such that the optimal control policy for the reduced-order model is the "best" suboptimal control policy for the actual system. The model reduction and control design procedures are thus intertwined.

While these control-sensitive methods avoid the above-mentioned problems with open-loop model reduction, they do incur added off-line computational burden over the more standard techniques. The implementational form of the resultant controller, however, compares favorably with the standard techniques. Further discussion on these advanced methods is beyond the scope of this report.

e. Aircraft State Models

Models which have been developed and refined (for example by using the model reduction techniques described above) for application to the design of aircraft control systems vary widely, ranging from simple point-mass "quasi-steady"* representations to sophisticated high-order models which include deflections of the airframe. For control design purposes, the designer typically attempts to arrive at the simplest model which adequately represents the "control object" or "plant" being addressed. This will usually result in the least expensive design in terms of engineering effort and also of implementation costs. Moreover, simpler models frequently allow the designer to acquire more insight into the process being controlled, resulting from the paring away of variable and functional relationships which are of secondary importance to the achievement of the control objectives. However, it is good engineering practice to retain higher fidelity system models as well, and use these to check the design which was based on the simpler, more extensively approximated models.

While an extensive summary of aircraft modeling activities is beyond the scope of this report, a discussion of selected modeling techniques and approximations is presented in the Appendix, which comments specifically on six-degree-of-freedom aerodynamic modeling (see also Ref. 4); the quasi-steady approximation; and the energy-state approximation.

---

* The quasi-steady approximation neglects acceleration of the aircraft.

3. DESIGN APPROACHES

Many techniques have been developed to synthesize control systems in general and aircraft guidance and control systems in particular. These techniques are typically categorized as to whether they treat linear or nonlinear systems, time-varying or time-invariant systems, continuous or discrete systems, multivariable or single-input/single-output systems, etc. Additionally, techniques can be compared as to the performance criterion they are attempting to satisfy and the general structure of the resulting controller design.

The individual techniques can be organized into several general approaches, the following three of which will be discussed in the remainder of this section:

- Nonlinear Optimal Control
- Linear Optimal Control (Quadratic Synthesis)
- Classical Control

Perhaps the key distinction between overall approaches to aircraft guidance and control system design is whether the design approach requires a linear, time invariant system model. This is the case with the bulk of the classical techniques and with some of the model reduction procedures (modal decomposition) discussed above.

Fortunately, for many problems of interest in aircraft guidance and control, a quasi-static approximation can be made. This proceeds as follows. The time-varying state model after linearization is given by Eqs. (7, 8), which are repeated below:

$$\delta\dot{\underline{x}}(t) = A(t)\ \delta\underline{x}(t) + B(t)\ \delta\underline{u}(t) \tag{33}$$

$$\delta\underline{y}(t) = C(t)\ \delta\underline{x}(t) + D(t)\ \delta\underline{u}(t) \tag{34}$$

Often, the variations in the matrix elements are slow relative to the dynamics of the state variables themselves. In this case, a common engineering practice is to approximate the time-varying linear system by a series of time-invariant system models, each referred to a particular reference point or "flight condition." Separate designs are then based on each of the linear, time-invariant models, and the individual designs then aggregated in such a way as to cover the flight envelope, i.e., the full range of flight conditions addressed by the design. Typically, a sufficiently general controller structure is selected so that only the controller's parameters or gains need be "scheduled" or varied as a function of trajectory variables (e.g., dynamic pressure, Mach number, etc.) in order to effect the required aggregated design. Optimal control techniques, both linear and nonlinear, are not restricted to time-invariant systems, and consequently do not rely on the quasi-static assumption. This distinction will be evident in the remainder of this section.

a. Nonlinear Optimal Control

Presented here is a brief summary of the optimal control design approach. The summary addresses deterministic optimal control only, rather than stochastic control where random inputs and uncertainties in the system parameters are allowed. Emphasis is on the basic principles and motivations of the approach as applied to the aircraft guidance and control problem. Rigorous development is beyond the scope of this report; for a more detailed treatment of the subject, the reader is referred to Refs. 6, 13 and 14.

(1) System Model

The nonlinear system model addressed by the optimal control approach was developed above and can be expressed in the form:

$$\dot{\underline{x}}(t) = \underline{f}(\underline{x}(t), \underline{u}(t), t) \qquad (35)$$

with the initial condition $\underline{x}(t_o)$ given. As will be seen later, in the solution to the optimal control problem, this state dynamic relation is treated as a "constraint" which must be satisfied at every point along the solution trajectory.

(2) Performance Index

The crux of the optimal control design approach is the specification of an appropriate performance index (or cost functional) because the "optimality" of the resulting design only has meaning when referred to this performance criterion. The performance index must be posed in a suitably concise form so as to be economically solvable by mathematical techniques, yet it must be sufficiently general to encompass a number and diversity of design objectives. Such objectives might address the time, fuel, or energy to reach a target condition, the terminal errors, mean-squared error along a path, etc.

The form for the performance index which has evolved to meet these broad and often conflicting requirements is given by:

$$J \equiv \phi(\underline{x}(t_o),\ \underline{x}(t_f), t_o, t_f) + \int_{t_o}^{t_f} L(\underline{x}(t),\ \underline{u}(t), t)\ dt \quad (36)$$

The performance index, J, is a scalar function which is defined such that low values of J (the "cost") indicate "good" performance and high values of J indicate "bad" performance. As can be seen in the above expression, J incorporates any requirements on the initial or terminal state by means of the penalty function $\phi(\underline{x}(t_o), \underline{x}(t_f), t_o, t_f)$ and any state-variable constraints, control-variable constraints, and optimality criteria in the function $L(\underline{x}(t), \underline{u}(t), t)$, which accrues penalty over the entire time interval of interest $[t_o, t_f]$.

Table 1 illustrates the generality of the performance index form (Eq. (36)) for expressing the control objectives of several simple aircraft guidance and control problems. Other such examples are provided in Section III.

TABLE 1
EXAMPLES OF THE GENERALITY OF THE PERFORMANCE INDEX STRUCTURAL FORM

$$J = \phi(\underline{x}(t_o),\underline{x}(t_f),t_o,t_f) + \int_{t_o}^{t_f} L(\underline{x}(t),\underline{u}(t),t)dt$$

PROBLEM	J	ϕ	L	EXAMPLES
Minimum Time	$J = t_f - t_o = \int_{t_o}^{t_f} dt$	0	1	• Intercept of attacking aircraft and missiles • Slewing-mode operation of radar or gun system
Minimum "weighted" (by H) terminal errors	$J = [\underline{x}(t_f)-\underline{r}(t_f)]^T H [\underline{x}(t_f)-\underline{r}(t_f)]$	$\phi(\underline{x}(t_f))$	0	• Ballistic missile control • Rendezvous for cargo delivery
Minimum "weighted" (by R) control effort	$J = \int_{t_o}^{t_f} \underline{u}^T(t)R\underline{u}(t)dt$	0	$L(\underline{u}(t))$	• Minimum rate of fuel consumption for rocket engine
Optimal tracking of reference $\underline{r}$, weighted by Q	$J = \int_{t_o}^{t_f} [\underline{x}(t)-\underline{r}(t)]^T Q [\underline{x}(t)-\underline{r}(t)]dt$	0	$L(\underline{x}(t))$	• Slewing of radar or gun to track target • Maintaining aircraft near reference path

(3) End Conditions

To complete the formulation of the optimal control problem, one must consider the end conditions required to be met by the problem solution. In general, the initial and final states (end states) and the initial and final times (end times) can be defined by a vector of algebraic expressions:

$$\underline{\psi}(\underline{x}(t_o),\underline{x}(t_f),t_o,t_f) = o \tag{37}$$

Any of these end states and end times may be completely fixed, completely free (i.e., unconstrained), or related to other end conditions* (i.e., certain relationships between the states and times must be satisfied at the end conditions).

(4) Problem Formulation Summary

The optimal control problem may now be stated simplistically: Find the control $\underline{u}(t)$ which minimizes the performance index J (Eq. (36)) and conforms to prescribed terminal constraints $\underline{\psi}$ (Eq. (37)) while satisfying the system dynamical equations (Eq. (35)).

Before the problem formulation is complete, one must consider the assumptions which may be permitted in order to arrive at its solution. Typically, these assumptions relate to the differentiability of the functions ϕ, L, $\underline{f}$, and $\underline{\psi}$ and to the boundedness of the states $\underline{x}$ and controls $\underline{u}$. For the remainder of this discussion, it will be taken that all necessary assumptions for solution are met and that the states are unbounded but the controls are bounded. The allowance for bounded rather than unbounded controls is of importance, since most physical processes contain controls that are bounded. Some aerospace vehicle examples

---

* Another way of saying this is that the end conditions are located on a hypersurface or manifold.

are: minimum and maximum thrust of a propulsion system, minimum and maximum deflection of a thrust vector, maximum available control power, maximum thrust vector rotation rate, etc.

(5) Solution Techniques

Most of the multitude of solution techniques which have been developed to address the optimal control problem can be placed in the following two categories:

- Calculus of variations techniques
- Numerical techniques

Calculus of variations (notably the Pontryagin minimum principle [15]) techniques can be used to obtain a set of analytic expressions which constitute a set of necessary conditions for optimality. Numerical techniques are inherently iterative, but can be used to converge on the optimal control time function and associated optimal trajectory over the time interval $[t_o, t_f]$.

There are many and varied numerical iterative techniques (e.g., the gradient method and quasi-linearization method, Ref. 14, Chapter 7; differential dynamic programming, Ref. 16; among others) further treatment of these is beyond the scope of this report. Because of its widespread use and the insight it lends into the nature of solution of the optimal control problem, however, the "minimum principle" approach will be summarized below.

(6) Minimum Principle

Solution by the minimum principle involves first augmenting the performance index by the mathematical technique of adjoining the constraints (Eqs. (35) and (37)) to the performance index J. This effectively converts the original constrained problem to an unconstrained problem of higher dimension. The "increase in dimension" is due to the use of Lagrange multiplier (adjoint) vectors $\underline{\nu}$ and $\underline{\lambda}(t)$. The adjoined performance

J* index is:

$$J^* = J + \underline{\nu}^T \underline{\psi} + \int_{t_o}^{t_f} \underline{\lambda}^T (\underline{f} - \dot{\underline{x}})\, dt \tag{38}$$

which, using Eq. (36), can be written:

$$J^* = \phi + \underline{\nu}^T \underline{\psi} + \int_{t_o}^{t_f} (L + \underline{\lambda}^T \underline{f} - \underline{\lambda}^T \dot{\underline{x}})\, dt \tag{39}$$

The adjoined performance index may finally be written in the more concise form:

$$J^* = \phi + \int_{t_o}^{t_f} (H - \underline{\lambda}^T \dot{\underline{x}})\, dt \tag{40}$$

by defining the Mayer functional:

$$\Phi(\underline{x}(t_o), \underline{x}(t_f), t_o, t_f) = \phi(\underline{x}(t_o), \underline{x}(t_f), t_o, t_f) + \underline{\nu}^T \underline{\psi}(\underline{x}(t_o), \underline{x}(t_f), t_o, t_f) \tag{41}$$

and the Hamiltonian:

$$H(\underline{x}(t), \underline{u}(t), \underline{\lambda}(t), t) = L(\underline{x}(t), \underline{u}(t), t) + \underline{\lambda}^T \underline{f}(\underline{x}(t), \underline{u}(t), t) \tag{42}$$

The minimum principle now determines the control which minimizes J* of Eq. (40) by examining the variation in J* (i.e., δJ^*) due to variations in the control ($\delta \underline{u}$). An extremum (i.e., a minimum under the desired circumstances) is reached where $\delta J^* = 0$

for arbitrary $\delta\underline{u}$. This requirement leads directly (Ref. 14, Chapter 2) to the Euler-Lagrange equations:

$$\dot{\underline{\lambda}}^T = - \frac{\partial H}{\partial \underline{x}} \tag{43}$$

$$\frac{\partial H}{\partial \underline{u}} = 0 \tag{44}$$

Equation (43) is also called the "adjoint" or "co-state" equation, since it describes the dynamics of the adjoint (or co-state) vector $\underline{\lambda}(t)$. The optimal control $\underline{u}_{opt}(t)$ is found from Eq. (44) if the control set is unbounded (unconstrained). For a restricted control set, alternate procedures must be used to find the control which minimizes the Hamiltonian* (Ref. 17, Section 4.3).

The minimum principle also determines expressions for boundary or transversality conditions necessary in the total solution. These expressions vary as a function of the "freedom" in the end conditions for $\underline{x}$ and t, as specified in the problem formulation. For example, if there are no terminal constraints $\left(\underline{\psi}(t_f) = 0\right)$ and the terminal time is a fixed rather than free value, the transversality condition is:

$$\underline{\lambda}(t_f) = \left(\frac{\partial \Phi}{\partial \underline{x}}\right)^T \Bigg|_{t=t_f} \tag{45}$$

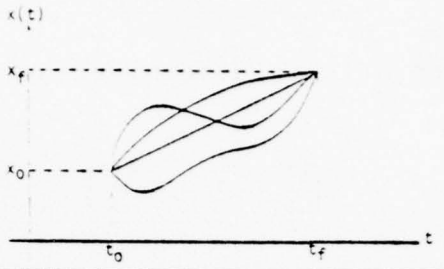
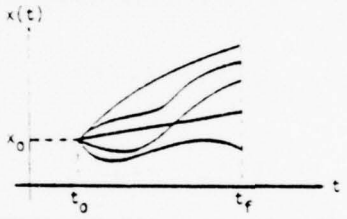
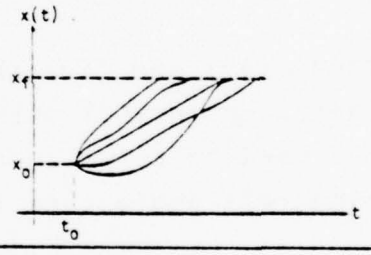
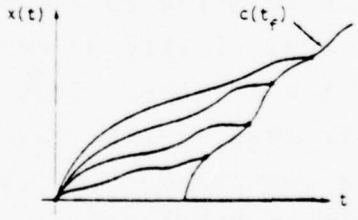
A summary of some of the more common end conditions and the corresponding transversality conditions are illustrated in Table 2.

(7) Comments

The minimum principle approach, while it yields valuable insight into the optimal control problem by providing analytical expressions for optimality, is not without practical difficulties. Many of these difficulties stem from the usual

* i.e., Eq. (44) will yield an expression for the control which minimizes the Hamiltonian if the control set is unbounded.

TABLE 2
ILLUSTRATION OF TYPICAL END CONDITIONS AND
ASSOCIATED TRANSVERSALITY EXPRESSIONS

DESCRIPTION	END CONDITIONS	TRANSVERSALITY	ILLUSTRATION OF ACCEPTABLE TRAJECTORIES
Fixed End Conditions	Fixed t_0 Fixed t_f Fixed $\underline{x}(t_0)$ Fixed $\underline{x}(t_f)$	–	
Free Terminal State	Fixed t_0 Fixed t_f Fixed $\underline{x}(t_0)$ Free $\underline{x}(t_f)$	$\underline{\lambda}^T(t_f) = \frac{\partial \phi}{\partial \underline{x}}\Big\|_{t_f}$	
Free Terminal Time	Fixed t_0 Free t_f Fixed $\underline{x}(t_0)$ Fixed $\underline{x}(t_f)$	$\frac{\partial \phi}{\partial t} + \underline{\lambda}^T \underline{f} + L \Big\|_{t_f} = 0$	
Terminal Time Unspecified But Related to Terminal State	Fixed t_0 Fixed $\underline{x}(t_0)$ $\underline{x}(t_f) = \underline{c}(t_f)$	$\left((\dot{\underline{c}} - \dot{\underline{x}}) \frac{\partial \phi}{\partial \underline{x}} + \phi\right)\Big\|_{t_f} = 0$	

occurrence of "split" boundary conditions of the differential equations which must be solved to obtain the optimal control. This two-point boundary-value problem is illustrated by summarizing the above development as follows: To find the optimal control, one must solve the following differential equations:

$$\dot{\underline{x}} = \underline{f}(\underline{x},\underline{u},t) \tag{46}$$

$$\dot{\underline{\lambda}} = -\left(\frac{\partial H}{\partial \underline{x}}\right)^T = -\left(\frac{\partial \underline{f}}{\partial \underline{x}}\right)^T \underline{\lambda} - \left(\frac{\partial L}{\partial \underline{x}}\right)^T \tag{47}$$

where $\underline{u}(t)$ is determined by

$$\frac{\partial H}{\partial \underline{u}} = 0 = \left(\frac{\partial \underline{f}}{\partial \underline{u}}\right)^T \underline{\lambda} + \left(\frac{\partial L}{\partial \underline{u}}\right) \tag{48}$$

subject to the boundary conditions, for example,

$$\underline{x}(t_o) \text{ given} \tag{49}$$

$$\underline{\lambda}(t_f) = \left(\frac{\partial \Phi}{\partial \underline{x}}\right)^T \tag{50}$$

Equations (49) and (50) constitute the split boundary conditions. In general, numerical methods or approximate analytical methods must be used to solve such a problem, namely, to integrate Eqs. (46) and (47) subject to the boundary conditions (49) and (50).

The solution to the nonlinear optimal control problem (found either analytically or numerically) is usually expressed simply as a function of time. Thus it can be pre-computed off-line, stored, and retrieved on-line and applied as necessary. Consequently, the optimal control $\underline{u}_{opt}(t)$ is an "open-loop" control. It is based entirely on the a priori model of the system (Eq. (46)); the optimal control does not require (or, more to the point, admit) measurements of the state at any time other than the initial condition $\underline{x}(t_o)$. As a result, the optimal control is not sensitive to deviations of the actual state from that predicted by the model, which may contain errors or approximations. Moreover, the optimal control is not sensitive to unmodeled disturbances which may

further drive the system states away from their modeled behavior. This open-loop nature of the optimal control is illustrated in Figure 10.

One way of dealing with these problems is to close the loop in effect by re-computing the optimal control periodically, using the current best estimate of the state (derived from the feedback sensors) as the initial condition for the most recent solution. This technique, while providing a closed-loop feedback control, can be extremely resource consuming, depending on the complexity of the control calculation and the repetition frequency required to satisfy closed-loop control objectives.

Under certain circumstances, it is possible to derive a closed-loop feedback form for the optimal control law directly, i.e., the control $\underline{u}$ can be expressed as a function of the state $\underline{x}$:

$$\underline{u} = \underline{u}(\underline{x}) \tag{51}$$

In this way, the current best estimate of the state can be used to calculate the current best value of control to be applied, as illustrated in Figure 11. The motivations for this state feedback control law and some conditions under which it can be obtained are discussed in the next section.

b. Linear Optimal Control

A large and important class of problems for which an optimal feedback control law, $\underline{u} = \underline{u}(\underline{x})$, can be found directly is that characterized by a linear system model and a performance index whose elements are quadratic forms. Under these conditions, a <u>linear feedback</u> control law can be found; i.e., the variational control $\delta\underline{u}$ is a <u>linear</u> function of the variational state $\delta\underline{x}$:

$$\delta\underline{u}(t) = -K(t)\delta\underline{x}(t) \tag{52}$$

where the linear gain matrix $K(t)$ can be pre-computed and stored. The on-line, instantaneous control is calculated by retrieving the current value of $K(t)$ from memory and merely multiplying by the current best estimate of the state $\underline{x}$. The method of deriving this optimal linear feedback control law is called "linear-quadratic" design or "quadratic synthesis."

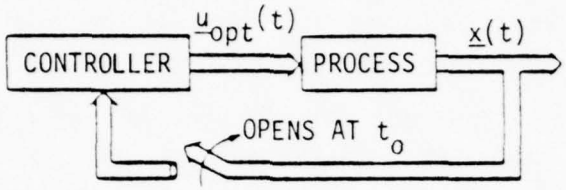


Figure 10. Optimal Open-Loop Control – $\underline{u}_{opt}$ Is Calculated *a priori* and Stored

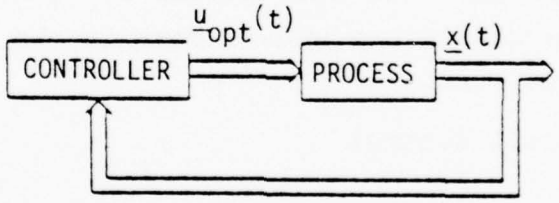


Figure 11. Optimal Closed-Loop Control – $\underline{u}_{opt}$ Is Calculated from State Feedback

(1) Quadratic Performance Index

The performance index to be minimized in order to derive the optimal linear feedback control law (Eq. (52)) is given by the following functional form:

$$J = \frac{1}{2}\delta\underline{x}^T(t_f)\ S_f\ \delta\underline{x}(t_f) + \frac{1}{2}\int_{t_o}^{t_f}\Big(\delta\underline{x}^T(t)\ Q(t)\ \delta\underline{x}(t) + \delta\underline{u}^T(t)\ R(t)\ \delta\underline{u}(t)\Big)dt \qquad (53)$$

where

S_f is an n×n weighting matrix on the terminal state error

$Q(t)$ is an n×n weighting matrix on the along-path state error

$R(t)$ is an m×m weighting matrix on the control deviation from nominal

S and Q must be at least positive semi-definite and R must be positive definite in order to obtain the desired form of the control law. Q and R can be functions of time; all matrices, if they depend explicitly on system states $\underline{x}(t)$ or controls $\underline{u}(t)$, are evaluated at the reference values $\underline{x}_o(t)$ and $\underline{u}_o(t)$.

There are two compelling reasons for choosing the quadratic form for the performance index. One of these, as will be seen shortly, is that the mathematics of solving the split boundary condition problem is greatly simplified. A more satisfying reason, however, derives from the model linearization process as presented previously. As shown in Eqs. (5) and (6) and repeated

below, the linearization process entails expanding the nonlinear model in Taylor Series about the reference values $\underline{x}_o$ and $\underline{u}_o$:

$$\underline{f}\left(\underline{x}(t),\ \underline{u}(t)\right) = \underline{f}\left(\underline{x}_o(t),\ \underline{u}_o(t)\right) + \left.\frac{\partial \underline{f}}{\partial \underline{x}}\right|_o \delta\underline{x}(t) + \left.\frac{\partial \underline{f}}{\partial \underline{u}}\right|_o \delta\underline{u}(t) + \underline{\alpha}_o\left(\delta\underline{x}(t),\ \delta\underline{u}(t)\right) \qquad (54)$$

$$\underline{g}\left(\underline{x}(t),\ \underline{u}(t)\right) = \underline{g}\left(\underline{x}_o(t),\ \underline{u}_o(t)\right) + \left.\frac{\partial \underline{g}}{\partial \underline{x}}\right|_o \delta\underline{x}(t) + \left.\frac{\partial \underline{g}}{\partial \underline{u}}\right|_o \delta\underline{u}(t) + \underline{\beta}_o\left(\delta\underline{x}(t),\ \delta\underline{u}(t)\right) \qquad (55)$$

The linear model retains the linear terms and neglects the higher-order terms $\underline{\alpha}_o$ and $\underline{\beta}_o$ in the expansion.

If these higher order terms are not forced to remain small, however, the validity of the first-order linear model can be jeopardized. Fortunately, it can be shown [5] that minimizing the quadratic performance index is equivalent to minimizing the magnitude (norm) of the higher order terms integrated over the time period of interest. Thus, the perturbation control $\delta\underline{u}$ based on the the quadratic performance index is the control which ensures the best linear model of the system being addressed. This is desirable because the <u>derivation</u> of the optimal perturbation control is based on the linear model <u>itself</u>.

(2) Linear-Quadratic Problem and Its Solution

In summary, the linear-quadratic problem is to find the perturbation control $\delta\underline{u}$ which minimizes the performance index given by Eq. (53) for the linear, time-varying system

$$\delta\dot{\underline{x}}(t) = A(t)\delta\underline{x}(t) + B(t)\delta\underline{u}(t) \tag{56}$$

The initial condition $\underline{x}(t_o)$ is given, the final time is fixed at the value t_f, and both the perturbation states and perturbation controls are unconstrained.

Solution of the linear-quadratic problem by the backward sweep method is well known (Ref. 14, Chapter 5; Ref. 17, Section 5.1). The solution is:

$$\delta\underline{u}(t) = - K(t)\ \delta\underline{x}(t) \tag{57}$$

where the m×n feedback gain matrix is given by:

$$K(t) = R^{-1}(t)B^T(t)S(t) \tag{58}$$

and $S(t)$ is the Riccati matrix, which is found by solution of the Riccati differential equation:

$$\begin{aligned}\dot{S}(t) = &- S(t)\ A(t) - A^T(t)\ S(t) - Q(t) \\ &+ S(t)\ B(t)\ R^{-1}(t)\ B^T(t)\ S(t)\end{aligned} \tag{59}$$

The Riccati equation is integrated backwards in time from the terminal boundary condition:

$$S(t_f) = S_f \tag{60}$$

Implementation of this solution (Eqs. (57) through (60)) can be quite simple in terms of <u>on-line</u> computational requirements. Often, only Eq. (57) need be computed on-line. This is the case when the references $\underline{x}_o(t)$ and $\underline{u}_o(t)$ are known for all time in the

interval of interest (see Figure 12). It is also the case when none of the matrices involved in the solution (namely, A, B, Q, R and S_f) depend explicitly on the reference trajectory and control.

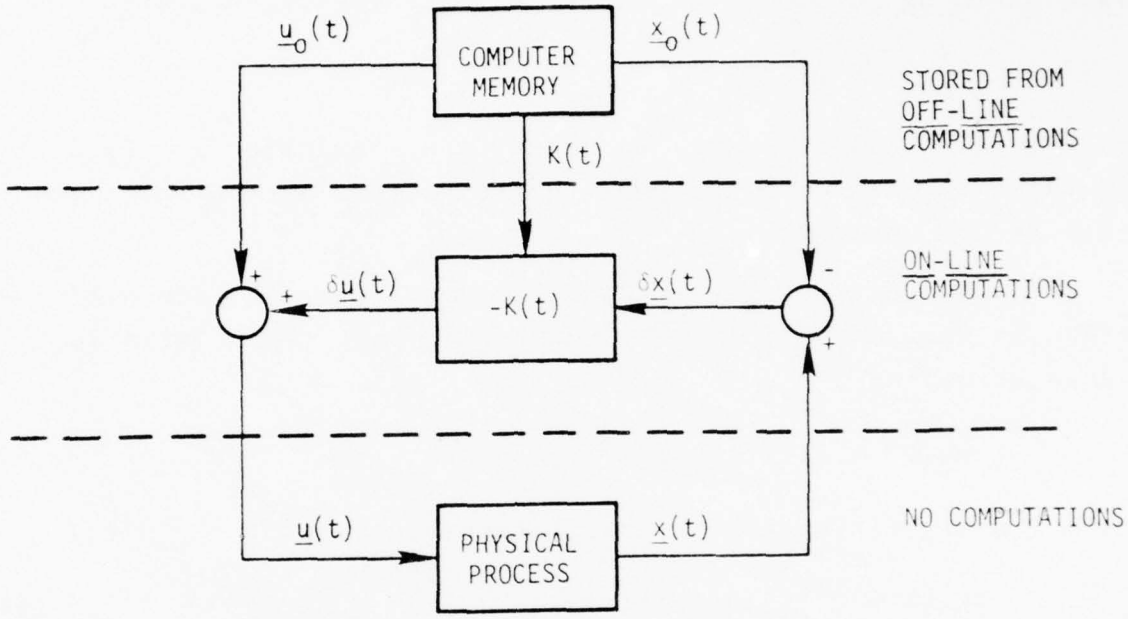


Figure 12. Illustration of Minimal On-Line Computational Requirements When Reference State and Reference Control Can Be Pre-Calculated

This will not always be the case, however, and the designer is left with two main choices:

1) Re-solve on-line for the gain matrix (Eqs. (58) and (59)) periodically as reference variables change; or

(2) Solve the problem off-line for a number of reference conditions and store K in a "schedule" as a function of these reference conditions; on-line computation then involves looking-up the proper gain from a table* (perhaps a multi-dimensional table) and making the multiplication of Eq. (57).

---

* This latter approach is similar to the quasi-static gain-scheduling technique used frequently in classical designs.

Various trade-off studies can be performed to determine which of these choices results in the most favorable combination of performance and computational load.

(3) Quadratic Synthesis

Quadratic synthesis refers to the process of formulating, solving, and implementing the linear-quadratic design. Activities which the engineer may have to perform in this overall design are listed in Figure 13. Also shown in the figure are various iterations which may occur in the design process to arrive at the proper final compromise between performance capability and implementational cost, in terms of engineering effort and computational hardware and software requirements.

The main thrust of quadratic synthesis, however, is the selection and refinement of the weighting matrices S_f, $Q(t)$, and $R(t)$ in the performance index. The selection of these matrices determines the character of the closed loop control, much as frequency response shaping can determine the character of a classical design. Similarly, the refinement of the weighting matrices is an iterative process, requiring a certain amount of experience and engineering judgment. However, the weighting matrices provide a great deal of insight into the design of complex, coupled, multivariable systems. As a result of this insight, many "rules of thumb" [5] have evolved for the design of large classes of aerospace systems. A few of These are summarized below:

1) Often a good choice (at least initially) of the weighting matrices is a diagonal form where the elements along the diagonal are inversely proportional to the square of the maximum desirable value of the quantity in question; or, mathematically, if q_{ij}, r_{ij} and s_{ij} are the elements of Q, R and S_f:

$$q_{ij} = 1/[x_{max}(t)]_i^2 \quad \text{if } i = j; \quad 0 \quad \text{if } i \neq j \qquad (61)$$

$$r_{ij} = 1/[u_{max}(t)]_i^2 \quad \text{if } i = j; \quad 0 \quad \text{if } i \neq j \tag{62}$$

$$s_{ij} = 1/[x_{max}(t_f)]_i^2 \quad \text{if } i = j; \quad 0 \quad \text{if } i \neq j \tag{63}$$

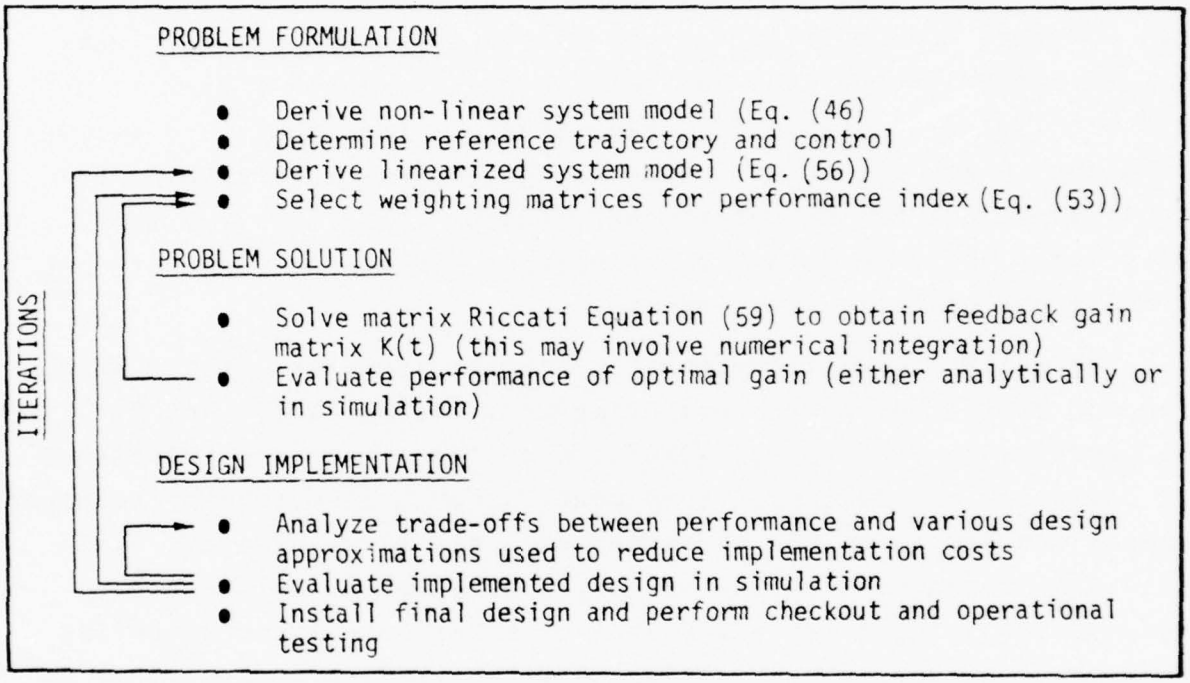


Figure 13. Typical Design Activities in the Formulation, Solution, and Implementation of the Linear-Quadratic Design

Another candidate initial choice, one which relates approximately to minimizing the second variation in J, is:

$$Q(t) \sim \left.\frac{\partial^2 H}{\partial \underline{x}(t)^2}\right|_o \tag{64}$$

$$R(t) \sim \left.\frac{\partial^2 H}{\partial \underline{u}(t)^2}\right|_o \tag{65}$$

$$S_f \sim \frac{\partial^2 \phi}{\partial \underline{x}(t_f)^2} \tag{66}$$

where ϕ is the Mayer functional (Eq. (41)) and H is the Hamiltonian (Eq. (42)) and the subscript (o) refers to the reference trajectory.

2) The larger the norm of the matrix S_f (i.e., $||S_f||$), the larger the gain matrix K(t) at times near the final time. Thus, as the final time approaches, certain elements of the control vector may get (unacceptably) large. One way of dealing with this problem is to gradually bring $||Q(t)||$, which penalizes state deviations along the path, to a magnitude comparable with S_f when nearing t_f.

3) The larger $||Q(t)||$, the larger the gain matrix K and the shorter the time period in which state perturbations are reduced to small values. In effect, increasing $||Q(t)||$ increases the bandwidth of the closed-loop system.

4) The larger $||R(t)||$, the smaller the gain matrix K and the slower the system response.

5) Frequently, the perturbation state vector contains variables and also their time derivatives (e.g., pitch angle and pitch rate). In such a case, penalizing by Q the pitch angle only and not its rate of change will lead to a more oscillatory response. Penalizing the pitch rate also will reduce overshoots and lead to a less oscillatory response. This is akin to increasing the damping coefficient of a second-order system.

c. Comparison to Classical Methods

As mentioned previously, classical methods normally address only a subset of the systems previously considered, namely, the subset known as linear, time-invariant systems. Such systems are characterized by constant-coefficient differential equations. This permits the formation of output/input transfer functions and the transform analysis of such relations by frequency domain methods (Bode Diagrams, Nichols' Charts, etc.). When applicable, such methods yield valuable information about the character of the system, which can be used to evaluate and improve control system designs. Even if a linear, time-invariant, quadratic synthesis method is applied to the design of particular control system, it is good engineering practice to check and analyze the resulting design using classical methods wherever possible.

The remainder of this section compares various aspects of the classical design methods with corresponding elements of the optimal control approach.

(1) Comparison of System Structure

Optimal control theory distinguishes between the control $\underline{u}$, state $\underline{x}$, and measurement $\underline{y}$ of a linear system. Again, the system parameters may be time varying. Classical control theory distinguishes only between the control (input) $\underline{u}$ and the measurement (output) $\underline{y}$ of the linear system. The system parameters are constant. An illustration of the two basic system structures is provided in Figure 14.

(2) Comparison of Design Criteria

Optimal control theory minimizes an index of system performance in the time domain. The index contains both constant and time-varying weighting matrices that, to a large extent, can be chosen freely. The elements of these matrices have a rather direct

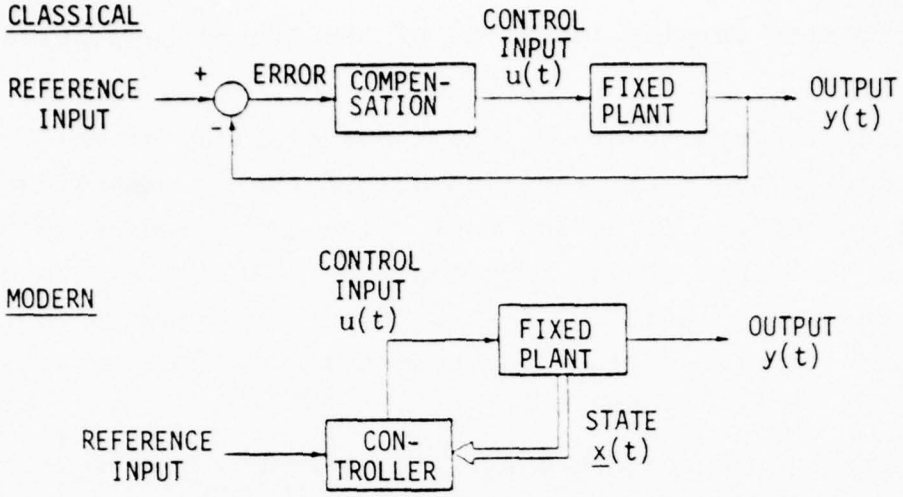


Figure 14. Comparison of the Basic System Structures of Classical and Optimal Control Theory (Example: Single-Input/Single-Output)

physical interpretation. The final time of the (transient) response may be prescribed arbitrarily, and requirements on the final state can be incorporated.

Classical control theory defines the "desired," fixed, closed-loop pole locations, associated with "desirable" system response. However, the relation between closed-loop pole locations and system response becomes more obscure as the system becomes more complex (multi-input/multi-output). Also, the relation between closed-loop pole locations and system response is not unique: the location of the closed-loop zeroes is also of importance. Final time of the response is fixed at infinity, since the main interest is really in steady state behavior [13].

(3) Comparison of the Control Law

Optimal control theory, as applied to the quadratic performance index, leads directly to a linear feedback law with time-varying gains. In general, all elements of the (n-dimensional) state vector are to be fed back to all controls. The time-varying

gains lead to time-varying locations of the closed-loop poles and zeroes.

Classical control theory assumes control to be of the linear, output-feedback type, i.e., the elements of the (m-dimensional) measurement vector are to be fed back. The gains are assumed to be constant. They are chosen such that the "desirable" closed-loop pole locations are obtained. If this objective cannot be met, then "compensation techniques" (cascade compensation; feedback compensation) are used to help achieve it.

The classical approach's use of the m-dimensional (external) measurement vector for feedback instead of the n-dimensional (internal) state vector leads, in general, to less satisfactory response, since the measurement vector contains less information about the system than does the full state estimate. However, a significant computer resource is required to "estimate" the full system state from a reduced number of noisy measurements. Fortunately, modern airborne computing systems are well capable of this state re-construction (by Kalman filter's, for example); this fact helps make the full state feedback design viable.

SECTION III
PATH CONTROL SYSTEM DESIGN

1. INTRODUCTION

A number of aircraft guidance and control problems have been addressed by the design approaches summarized in Section II. Typically, the overall aircraft guidance and control task is broken down into a number of subproblems (navigation, horizontal guidance, stability augmentation, etc.) and each of these addressed by design techniques which are best suited to the characteristics and design objectives of the particular subproblem. The diverse subsystem designs are then integrated, sometimes in a rather ad hoc manner, to arrive at the total aircraft guidance and control system design.

There is good reason for this process of decomposing the large, complex problem of guidance and control. Primarily, the high dimensionality and high degree of nonlinearity exhibited by the overall problem does not permit direct solution for an implementable design. Moreover, the widespread success in developing practical flight control systems by integrating the individual subsystem designs is strong indication that blind application of any particular technique to the full-dimensional problem is not warranted. However, it is important that the designer have a firm understanding of the interrelationship of the subsystems while he is designing any particular one. In this way, oversights and inconsistencies are minimized and the design integration process should proceed smoothly.

To assist in providing this insight into the interrelationship of guidance and control subsystems, this section defines a conceptual framework by which to partition the path control problem for discussion and analysis. The two main partitions

of this framework, reference generation and perturbation control, are then discussed separately.

2. SYSTEM PARTITIONING

Many aspects of aircraft guidance and control can be discussed within the path control framework illustrated in Figure 15. This conceptual diagram identifies two major partitions: 1) the reference generator, and 2) the perturbation controller. The reference generation function determines the "nominal" state (trajectory) and control which satisfy the outer-loop control objectives (guidance, performance optimization, etc.). The perturbation control function attempts to maintain the actual state near the nominal ("departure prevention") while simultaneously satisfying other inner-loop control objectives (disturbance rejection, stability augmentation, etc.). The perturbation control is then added to the nominal control to form the total control, which is sent to the actuation system.

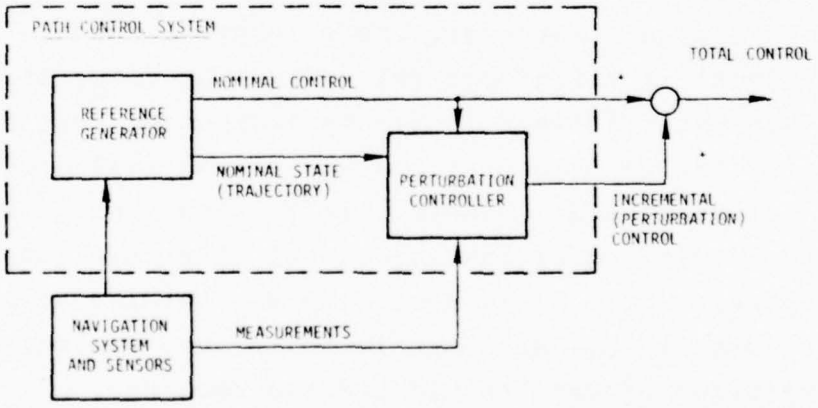


Figure 15. Generic Block Diagram of a Path Control System

The basis for the structure illustrated above lies in the nature of the linearization process (as discussed in Section II) and in the related concept of "neighboring path" optimal control (Ref. 14, Chapter 6). In this concept, the reference solution addresses the full-scale, nonlinear system model to obtain the optimal "open-loop" control and associated optimal trajectory, which satisfies outer-loop control objectives. The perturbation control is then derived through linearizing about this reference solution and determining the linear feedback gains which minimize deviations from the reference.

In practice, the "pure" optimal path and neighboring optimal path problem is not generally addressed in full dimension. Rather, many simplifications and engineering approximations are made in the design process. These approximations lead to a suboptimal solution to the overall problem. Moreover, such approximations frequently obscure the interface between the two conceptual partitions of reference generation and perturbation control. For instance, the reference solution to the nonlinear, outer-loop problem (e.g. minimum time to climb) may make approximations which neglect fast dynamics (e.g. pitch angle and rate) and treat certain fast-varying system states (e.g. flight-path angle) as "artificial" controls. The output of the outer-loop problem solution now consists of some of the reference states (e.g. altitude and velocity) and "artificial" control variables (e.g. flight path). Before this problem can be cast in the path-control framework (Figure 15), nominal values must be computed for the remaining reference states and the true reference control (e.g. a "trim" elevator and nominal thrust history which are consistent with the reference velocity must be computed). Often it is convenient to locate such computations (e.g. elevator trim) with the inner-loop control functions, i.e. within the perturbation

control partition. Notwithstanding such exceptions, the path-control formal structure defined above is a valid and helpful context within which to view the design of the overall system, as demonstrated in the remainder of this section.

3. REFERENCE GENERATION

As defined above, reference generation addresses outer-loop control objectives, of which there are two general categories: (1) performance optimization and (2) guidance. The distinction between these two classes is that performance optimization is not generally concerned with geographic position, but rather with the time-optimal or fuel-optimal maneuvers or transitions between energy states. Guidance, on the other hand, is primarily concerned with position attainment, and performance optimization is viewed as a secondary objective.

Many types of performance optimization are of major significance only for supersonic or fighter aircraft. Such problems include minimum-time and minimum-fuel climbs, dives, and turns. A survey of literature describing the application of optimal control theory to selected performance optimization problems is presented in Table 3. Such performance optimization problems are not considered further in this report in their "pure" form, but only as performance optimization relates to optimal guidance.

For transport aircraft, the guidance problem is conventionally divided into the horizontal and vertical planes. Horizontal guidance addresses the synthesis of trajectories which overfly prescribed waypoints or avoid hazardous geographic regions, both without and with control of the time at which various points on the trajectory are reached (time-of-arrival guidance). Vertical guidance is concerned with achieving time-optimum or fuel-optimum altitude/range profiles, with avoiding vertical

TABLE 3
SURVEY OF AIRCRAFT PERFORMANCE OPTIMIZATION LITERATURE

REFERENCE NO.	PROBLEMS ADDRESSED	COMMENTS
18	• Minimum time to climb (change energy level) • Minimum fuel to climb • Maximum range profiles	• Uses energy-state approximation and energy management techniques • Comparison of approximate and near exact solution • Numerical results for two representative supersonic aircraft
19	• Minimum time to gain energy • Minimum fuel to gain energy	• Compares singular perturbation approach to conventional energy management methods
20	• Minimum time loop maneuver	• Four-dimensional state model • Calculus of variations approach • Numerical results for typical high-speed jet aircraft
21	• Three-dimensional maneuvering--minimum-time transition from initial to final altitude, velocity, and heading	• Singular perturbation approach • Consider aircraft constraints (thrust maximum, g-limit, etc.) • Numerical example of F-4E engaging with F-106
22	• Three-dimensional minimum-time turns	• Numerical results for F-4H aircraft
23	• Three-dimensional minimum-fuel turns	• Numerical results for F-4H aircraft
24	• Minimum-time turns at constant altitude	• Numerical results for hypothetical supersonic airplane

threat contours, or with terrain following. If necessary, three-dimensional (or three-dimensional plus time) guidance objectives can be satisfied by integrating the horizontal and vertical designs. For example, the horizontal guidance solution for total path length can be used as input to the vertical guidance laws, which are then solved to determine the fuel optimum altitude/velocity profile to achieve this desired total range. The horizontal and vertical guidance problems are discussed separately below.

a. Horizontal Guidance

Horizontal guidance objectives, as a rule, stem from two higher-level concerns: (1) flight management and (2) threat avoidance. Flight management is concerned with the synthesis of trajectories which:

- pass through specified waypoints in a controlled manner
- transition from an initial location (waypoint) and heading to a final location (or location and heading)
- intercept and fly along a line in a specified direction.

Threat avoidance in the horizontal plane,* of course, is concerned with the avoidance of specified hazardous topographic regions within a given altitude range so as to minimize the exposure to threat or maximize the probability of mission success. In addition to these primary concerns, horizontal guidance objectives frequently include control over the time of arrival at specified points along the path, notably the terminal point.

---

* Strictly speaking, the threat avoidance problem is three-dimensional, involving the consideration of altitude as well as horizontal position in order to avoid the three-dimensional threat volumes. For illustration here, the horizontal aspects of the threat avoidance problem will be emphasized, with altitude assumed to be constrained within some acceptable range. The algorithm which generates the simulation results presented later, however, is capable of treating the full three-dimensional problem.

(1) Minimum-Time Transition

Most common problems in horizontal guidance can be classified into three types [25]:

Type 1: Flying from an initial point and heading to a specified final point and heading;

Type 2: Flying from an initial point and heading to intercept and then fly along a line of specified heading; and

Type 3: Flying from an initial point and heading to a specified final point with arbitrary final heading.

Many more complicated horizontal guidance problems can often be interpreted as a sequence of these basic problem types.

The solutions to the three guidance problems defined above are not unique; i.e., problem Type 1 may be solved by a number of steep turns and straight path sections or by a few sweeping turns. In the interest of being able to generate efficient and predictable trajectories for all initial and final conditions, it is reasonable to ask what trajectory performs the desired transition in minimum time.

In formulating the minimum-time optimal control problem, one typically uses the planar, point-mass aircraft model:

$$\dot{x} = v_x \tag{67}$$

$$\dot{y} = v_y \tag{68}$$

$$\dot{v}_x = -(f_\ell/m) \sin \psi \tag{69}$$

$$\dot{v}_y = (f_\ell/m) \cos \psi \tag{70}$$

where ψ is the heading angle measured clockwise from the x-axis, i.e.:

$$\psi = \tan^{-1} (v_y/v_x) \tag{71}$$

and where

x and y are the coordinates of position in the plane

v_x and v_y are the components of velocity in the plane

f_ℓ is the lateral force.

The lateral force f_ℓ can be considered to be the control, or else the bank angle ϕ can be used as the control, since the two are related by:

$$f_\ell = m\ g\ \tan\ \phi \tag{72}$$

By convention, positive ϕ corresponds to right wing down.

Realistically, the control variable must be constrained, either by specifying a minimum allowable turning radius R_{min}, maximum allowable bank angle ϕ_{max}, or maximum allowable lateral force $f_{\ell\ max}$. For constant velocity turns, these are related by:

$$R_{min} = V^2/(g\ \tan\ |\phi_{max}|) \tag{73}$$

$$f_{\ell max} = m\ g\ \tan\ |\phi_{max}| \tag{74}$$

where V is the total aircraft velocity magnitude.

The minimum-time transition can now be found by minimizing the Hamiltonian:

$$H = 1 + \lambda_1 v_x + \lambda_2 v_y + f_\ell/m\ (-\lambda_3 \sin\ \psi + \lambda_4 \cos\ \psi) \tag{75}$$

subject to the system equations (67-70) and control constraint equation (74). In the above equation, the λ's are the costates or LaGrange multipliers. The three types of guidance problems defined previously can be formulated by specifying appropriate final conditions on the state and costate.

As can be seen in Equation (75), the control variable enters linearly* in the Hamiltonian. Application of the minimum principle

---

* Rather than, say, quadratically as in the linear-quadratic (quadratic synthesis) problem described in Section II.

to such problems results in a so-called singular solution. This is evident since the necessary condition:

$$\frac{\partial H}{\partial u} = 0 = \lambda_3 \sin \psi - \lambda_4 \cos \psi \qquad (76)$$

does not result in expression solvable for the control f_ℓ in terms of the state and costate variables. Instead, for singular problems, the control is found by the requirement that Eq. (76) be satisfied for a finite amount of time; in other words, the time derivative of $\partial H/\partial u$ must be zero.

Carrying through the conventional techniques for solving such singular problems, it has been shown [25] that the non-singular intervals of trajectories consist of turns with maximum bank angle (and hence minimum allowable turning radius) and the singular intervals of optimum trajectories consist of straight-line flight. Specific optimal transitions for the three types of guidance problems described above can be synthesized from such maximum bank-angle turns and straight line segments, using certain heuristic rules to assure the attainment of prescribed end-points with a minimum amount of maneuvering.

Application of the above to the horizontal guidance problem takes on both off-line and on-line connotations. Off-line, of course, the theory can be used to synthesize particular flight plans to fly prescribed scenarios. In addition, on-line algorithms have been generated to synthesize minimum time or minimum path-length transition trajectories for end-point attainment. As an example, one such on-line algorithm [26], known to require about 10 milliseconds on a fixed-point Sperry 1819A computer for solution, has been successfully used for trajectory "capture" -- in particular for the minimum-time nulling of lateral errors which are typically discovered by an on-board guidance system when it acquires highly accurate microwave navigational data near the runway.

The outputs of the horizontal guidance trajectory generation, then, are the reference trajectory coordinates x_R, y_R and the reference bank angle ϕ_R, which is nominally zero in the straight segments or equal to $\pm\ \phi_{max}$ during turns. (Command smoothing or rate-limiting may also be used to "soften" these transitions in ϕ_R command between zero and ϕ_{max}.)

(2) Controlled Time of Arrival

As mentioned previously, guidance objectives frequently include controlled time of arrival at specified points along the synthesized reference path. Control over the time of arrival at an arbitrary point on the path can be exerted either by modification of the total path length up to that point, (e.g., path-stretching maneuvers) or by modulation of the aircraft speed. Again, as was the case with horizontal flight-path synthesis, an infinite number of solutions to the time of arrival problem exist. One solution practical for many flight management applications is discussed below.

The problem is to synthesize a speed profile for a given reference horizontal trajectory such that an aircraft starting with initial speed V_o at time t_o arrives as the final point at the specified time t_f with velocity V_f. The constraints are that the speed V must be within the range of the minimum (V_{min}) and maximum (V_{max}) speed restrictions of the aircraft and that speed changes must be carried out with constant acceleration A_a or deceleration A_d, selected to fit the performance of a particular aircraft.

A particular practical algorithm [27] for solving the problem posed above is described below. The solution is broken down into three steps.

First, the algorithm tests the feasibility of the reference path length L by comparison with L_{max} and L_{min}, which are the maximum and minimum distances the aircraft is capable of traversing in the allotted time, respectively. If the path length exceeds

L_{max}, the speed profile is beyond the aircraft's performance capability of flying, and a later arrival time must be specified. If the path length is less than L_{min}, it must be increased so that the new path length is within the range of L_{min} to L_{max}, for instance by using a path-stretching maneuver.

Second, the algorithm defines an appropriate speed profile consisting of at most three segments: an acceleration or deceleration segment starting at V_o, a constant speed segment at some nominal speed V_n, and another acceleration or deceleration segment ending at V_f. The definition of the appropriate speed profile involves two additional parameters L_1 and L_2, which are defined respectively as the minimum and maximum distances that can be travelled in the allotted time interval <u>if speed is constrained</u> to lie between V_o and V_f. These parameters correspond to the shaded areas under the speed profiles shown in Figure 16. The parameters L_1 and L_2 are used to select an appropriate reference speed profile from the candidates shown in Figure 17. For example, if L less than L_1 (<u>and</u> if L passes the feasibility test in Step 1 above), the appropriate profile must include sustained flight at a nominal speed V_n lower than both V_o and V_f, as shown in the first curve in Figure 17.

Third, the numerical values of the parameters in the selected speed profile are determined by matching the area under the selected curve with the reference feasible path length L.

The output of this time-of-arrival control algorithm is a reference speed profile V_R, which may now be included with the horizontal guidance reference states x_R, y_R, and ϕ_R, as defined above.

(3) Threat Avoidance

A very promising area for the application of optimization theory is the problem of maximizing the probability of success of tactical missions subject to enemy threats. The

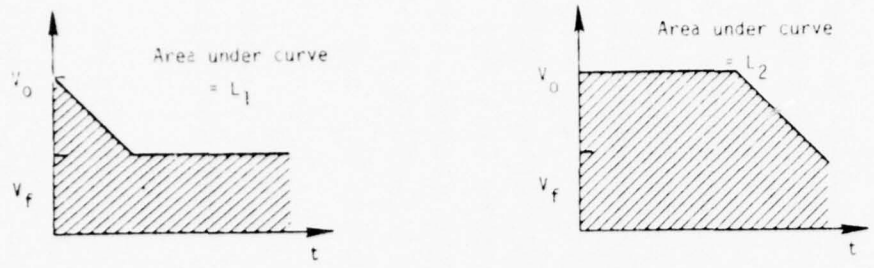


Figure 16. Definition of Path-Length Reference Parameter L_1 and L_2

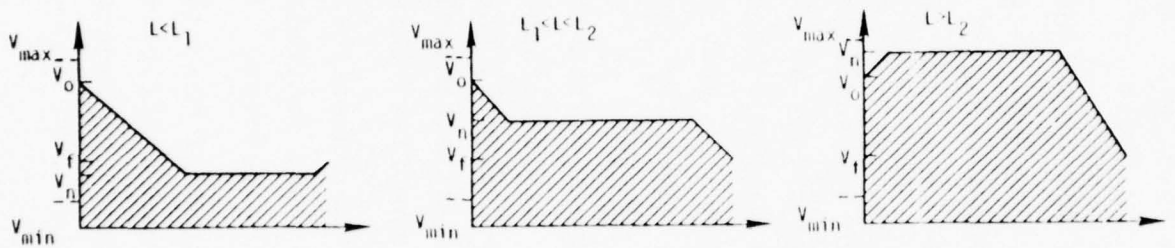


Figure 17. Candidate Profiles for Speed Control Algorithm

problem is twofold: (1) determining the optimal flight path through the threat environment, and (2) determining the optimal utilization of countermeasure resources so as to reduce threats along the selected path. Obviously and unfortunately, these two aspects of the problem are highly coupled: the optimality of the selected path in terms of mission success probability and probability of survival is strongly dependent upon how countermeasure resources are applied. Conversely, it is usually best to direct countermeasure resources so as to concentrate on paths which exhibit some degree of optimality in terms of fuel expenditure or total time of exposure to threats.

Many simplified approaches have been taken to the threat avoidance problem, with very limited success. The main difficulty lies in the high degree of dimensionality incurred by the strong coupling of the several important factors cited above. Simplifications which neglect certain factors can be sufficiently suboptimal so as not to be worthwhile.

One technique which is highly suited to such optimization processes is dynamic programming. Dynamic programming converts the problem to a multistage decision process; the control solution is formulated as the sequence of decisions which optimizes a multifaceted performance index over the entire trajectory. Basically, dynamic programming converts the simultaneous determination of the entire optimal control sequence into a tractable sequential solution of vastly simpler intermediate optimization problems.

Historically, dynamic programming solutions to high-dimensional problems have incurred severe computational requirements. Much of this difficulty stems from the use of conventional, direct algorithms which attempt to exhaustively search all possible control combinations. Innovative solution algorithms, however, have been developed to obviate the need for this exhaustive search. Moreover, advances in computer architectures, namely the advent of highly parallel array processors, ideally suit the dynamic

programming solution technique of decomposition into multiple subproblems. Consequently, a dynamic programming solution to the sophisticated threat avoidance problem is extremely feasible.

To illustrate the performance of a particular dynamic programming algorithm, results are presented below from some recent work [28] which generates optimum flight paths and countermeasure resource allocation for penetrating enemy defenses. The algorithm is capable of incorporating:

- Three-dimensional and flight direction dependence of the lethality of threats,
- Variation in fuel consumption as a function of speed and altitude,
- The effects of uncertainty in the existence and location of the threat,
- Terrain masking,
- Expendable Electronic Warfare (EW) resources (e.g., decoys, chaff, anti-radiation missiles)
- Non-expendable EW resources (e.g., radio frequency jamming)
- Variations of aircraft radar cross-section as a function of aspect angle,**
- Boundary conditions, such as requiring the aircraft to approach the target from a specific direction,
- Fuel constraints.

The algorithm will make the optimum tradeoff of available penetration techniques such as flying around threats, jamming, decoying, flying under radar coverage, etc., to determine the optimum means of penetration.

Figure 18 shows the symbology used in the simulation results which follow. As shown, the threats may either be known with certainty, or uncertainty may exist in their actual location*

---

* Additional "pop up" threats, which represent those detected during the mission by on-board sensors, can also be handled by the simulation model.

** I.e., the angle between the aircraft's plane of maximum cross-sectional area and the radar line-of-sight.

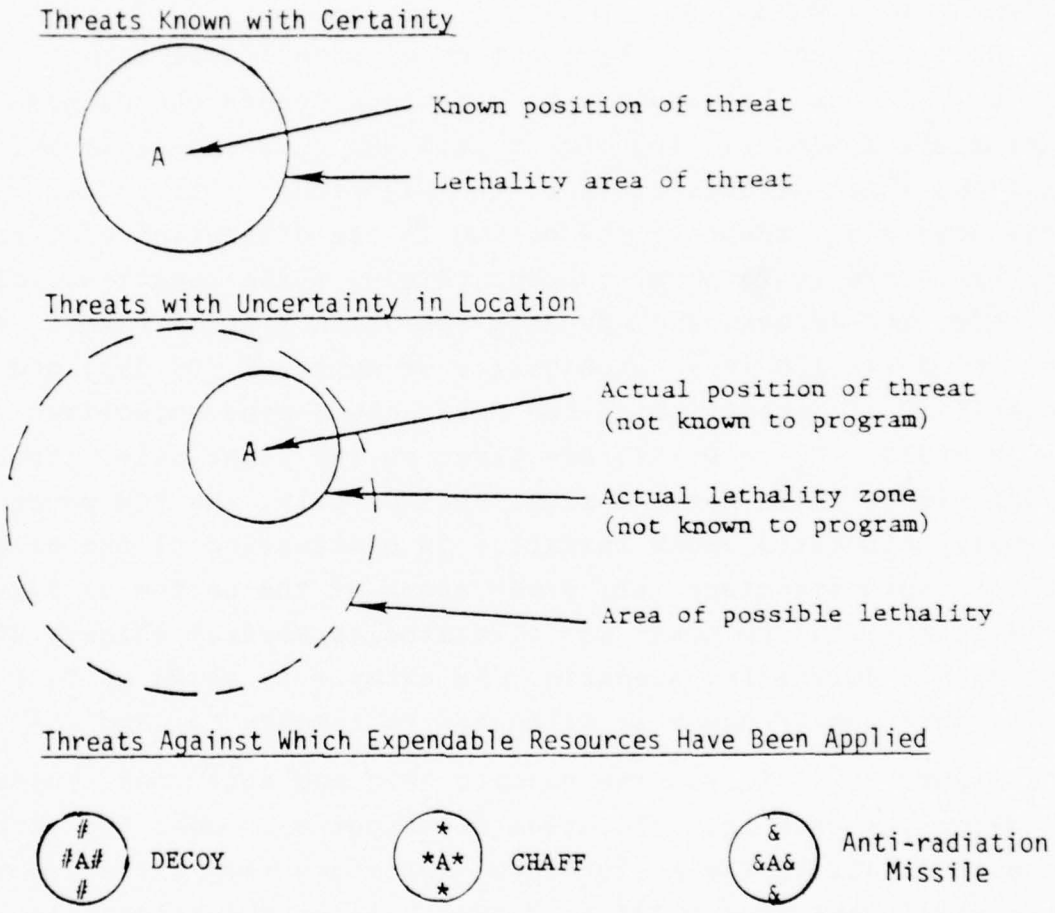


Figure 18. Symbology Used in Threat Avoidance Simulation Examples

(all threats are SAM sites). Threats against which expendable resources have been deployed are indicated as shown; such deployment, of course, serves to reduce the effectiveness of the threat.

An example run of a dynamic simulation developed to evaluate the threat avoidance algorithm is shown in Figure 19. The scenario seeks the attainment of two objectives T1 and T2 in the presence of thirteen threats: A1, A2, B1, B2, B3, B4, B5, B6, B7, C1, C2, C3, and C4. The location of some of the threats (A2, C1, C2, C3, C4) are not known with certainty, hence the dashed uncertainty contours. The flight path shown is the minimum-fuel solution, which is used to start the algorithm -- it is not the final solution. Shown at the bottom is the allocation of Electronic Countermeasure (ECM) power to each threat, three quantized values of chaff, two decoys, and one Anti-radiation Missile (ARM). The fuel used (11,750 lbs), probability of survival (0.738), and the probability of accomplishing the first and second objectives (P_{T_1} = 0.935, P_{T_2} = 0.774) are given on the right side. Even though Figure 19 is not the final optimum path, the ECM power is optimally allocated among threats. An examination of the allocation of radio frequency (RF) power shown at the bottom of Figure 19 indicates that RF power was allocated to several threats at many points during the scenario. An example is shown at time point 12:20 where the RF power is allocated to threats C3 and C4.

Figure 20 indicates the results obtained after the program optimizes the path and allocation of resources. Note the large increase in all of the performance indicators (e.g., the probability of survival went from 0.738 to 0.887). Also, the allocation of many of the expendables changed as was expected. One unit of chaff originally allocated to threat C1 was changed to A1 and the decoy allocated to B3 was reallocated to B1. All expendable EW resources are deployed and all of the available fuel is used. This occurs because allocating a resource results in increased performance compared to not allocating the resource; i.e. the cost penalty placed on actually using the allotted expendables is low compared to the cost penalty associated with mission failure.

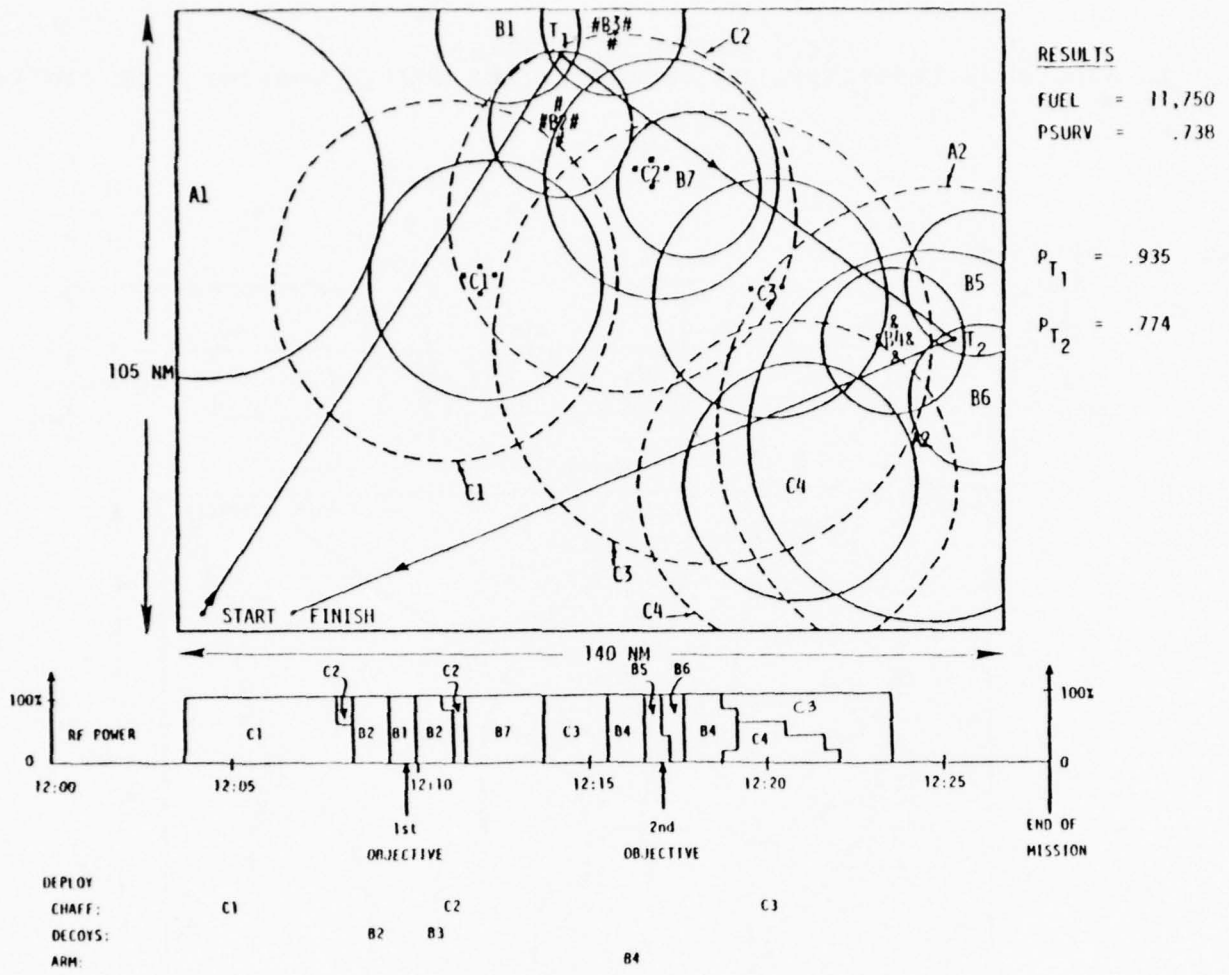


Figure 19. Simulation Results Summary for Example Threat Scenario and Minimum Path [28]

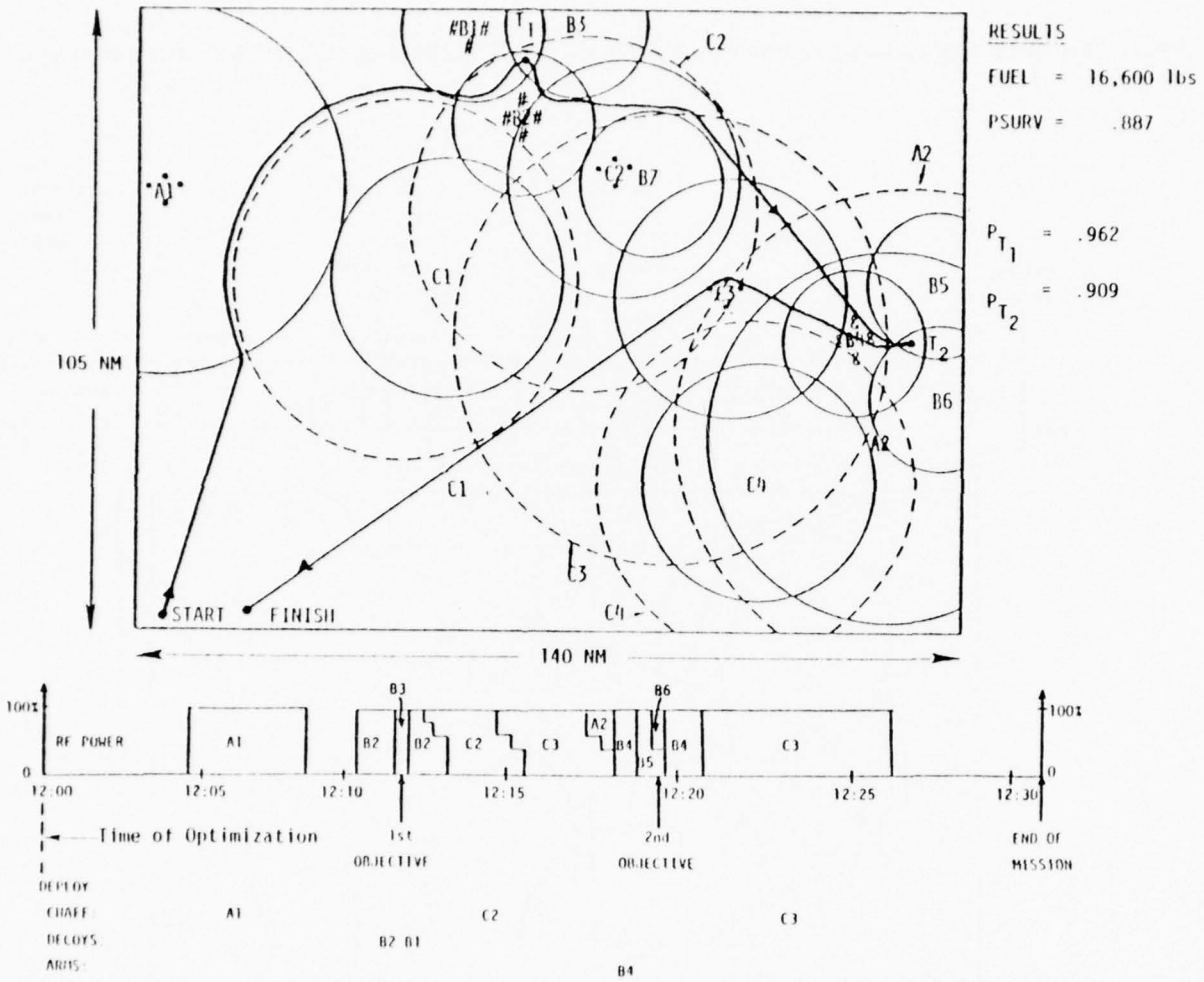


Figure 20. Optimum Flight Path Assuming No Additional Knowledge of Threats is Gained [28]

Thus far the optimum solutions have all been based on a priori (although probabilistic) information. Consequently, the optimum trajectory solutions could have been performed off-line and stored prior to the flight. If onboard sensors or a reconnaissance/communications system reduce uncertainty in threat location (or discover previously unknown threats), radically different solution trajectories and optimum allocations of resources result. Figure 21 presents such an example where on-line recomputation of the optimum solution is necessary. As shown, it is assumed that the aircraft has proceeded successfully to the point P, at which time onboard sensors determined the actual location of threat C1. This eliminates the uncertainty in C1's location as indicated by the removal of the dashed circle around C1. The new allocation of resources and flight path is shown. Since the flight path to objective T1 is more direct than in Figure 20, more fuel is available to fly around threats C2 and C3. This caused a reallocation of a decoy from B1 to B3 and a reallocation of chaff from C2 to A2. With this new allocation and flight path, the probability of survival increased to 0.897. Results of this nature were also obtained when previously unknown "pop-up threats were introduced.

Computer resource requirements for executing (on-line) the dynamic programming algorithm discussed above are not prohibitive. Even the direct-search, serial processing form as implemented on a Univac 1108 (1 μ sec cycle time) takes less than 8 minutes for complete solution. Using the implicit stage algorithm can reduce this to less than 8 seconds; however, this algorithm has the undesirable property of prohibiting transitions back toward the starting point. This difficulty is alleviated by other mathematical techniques, such as the method of successive approximations, which can obtain an approximate solution on a serial processor in about 10 seconds to a minute. Far greater speed improvements (1000/1 speed up) are possible if off-the-shelf parallel processors are employed. This occurs because the computations necessary to

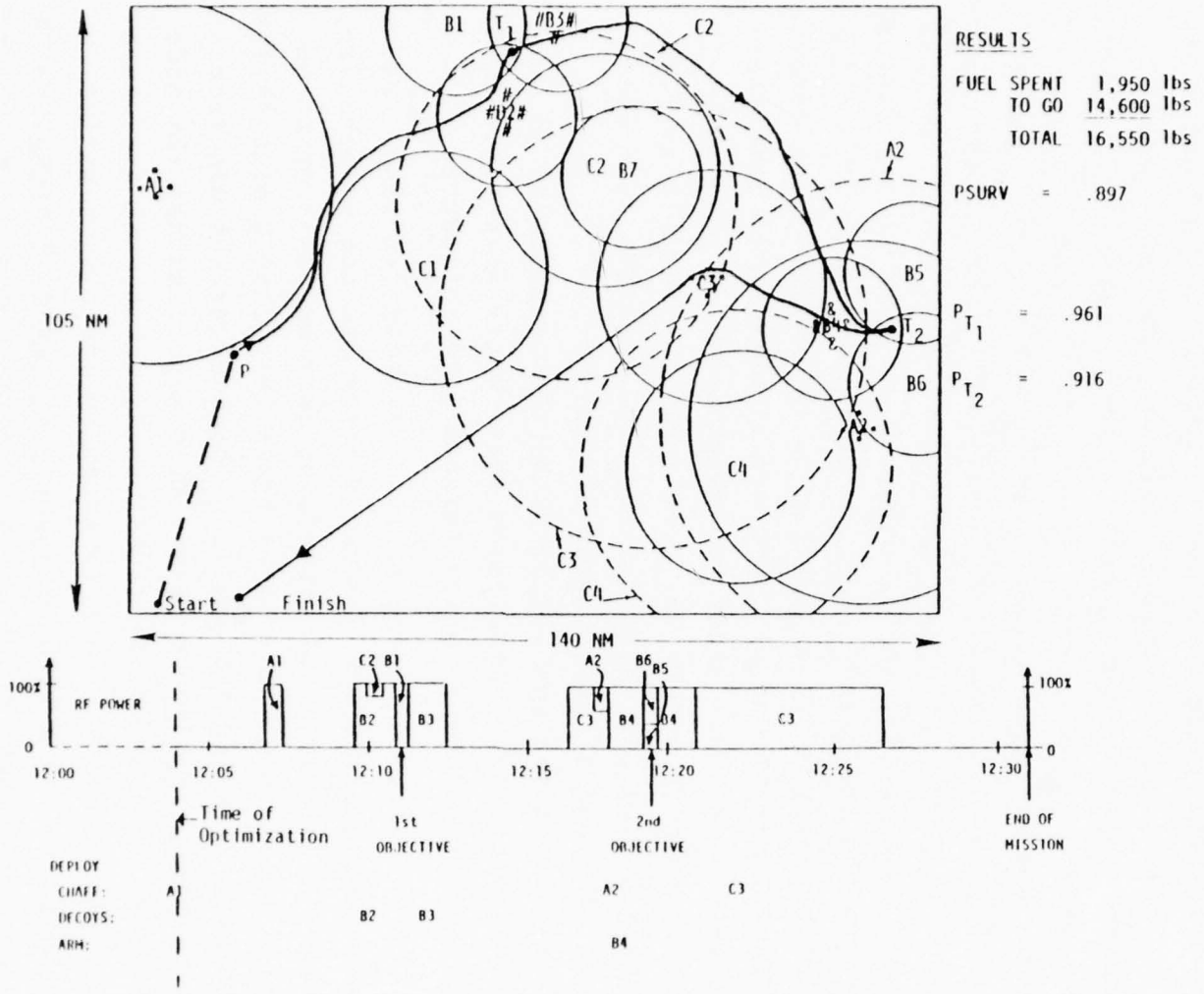


Figure 21. Optimum Flight Path Four Minutes Into the Flight Assuming Uncertainty in Threat C1 Eliminated Due to Onboard Sensors [28]

determine the optimum transition for all states at a given stage are independent of each other and, therefore, can be performed in parallel. Typically, the designer will use such a dramatic improvement in processing speed capability to obtain a more accurate solution while letting solution time approach some reasonable number (say 30 seconds). This is usually done by reducing the "granularity" of the solution, i.e., by breaking the optimization problem up into a greater number of stages.

The preceding has shown an implementable basis for reference generation in the horizontal plane which is an alternative to conventional two-dimensional horizontal guidance. The outputs to the inner loop are the same, however, namely the reference positions in the horizontal plane x_R and y_R and the velocity magnitude V_R. Nominal bank angles ϕ_R for required turns can also be synthesized by relating bank angle to turn radius R by using the relation:

$$R = V_R^2/(g \tan |\phi_R|) \tag{77}$$

b. Vertical Guidance

Typical objectives of aircraft guidance in the vertical plane are the generation of:

- Time-optimum or fuel-optimum altitude profiles to achieve a given altitude and/or range transition;
- Profiles to maximize range for a given thrust level and fuel allotment;
- Commands to follow terrain or avoid vertical threat contours while simultaneously optimizing other aspects of performance (e.g., minimum throttle activity).

A moderate amount of work has addressed optimal control solutions to these vertical guidance problems, notably Refs. [18], [19] and [29] through [32]. Most of the practical on-line implementations of these solutions derive from the application of the so-called "energy management (EM)" methods.

The EM methodology is characterized by order-reduction approximations to the point-mass longitudinal equations of aircraft motion. In particular, the energy state approximation (see Appendix) is used to eliminate the dynamic equations for velocity and flight path angle in favor of a single dynamic equation in the energy state:

$$\dot{E} = (T-D)V/m \tag{78}$$

where E is the total (sum of kinetic and potential) energy per unit mass, i.e:

$$E = 1/2\ V^2 + gh \tag{79}$$

and where

T is the thrust
D is the drag
V is the velocity magnitude
m is the mass
h is the altitude
g is the acceleration of gravity

Thrust is assumed to be a function of altitude (h), velocity, and throttle setting (π):

$$T = T(h,V,\pi) \tag{80}$$

and drag is a function of altitude and velocity:

$$D = D(h,V) \tag{81}$$

The other dynamic equations retained in the EM methodology are:

$$\dot{x} = V \tag{82}$$

$$\dot{m} = f(h,V) \tag{83}$$

where x is the along-track position coordinate and f is the fuel flow rate. In the equations above, both angle-of-attack and flight-path angle are considered small, and lift equals weight.

Before exploring some illustrative examples of the EM methodology, it is appropriate to note several important points:

- Certain problems are addressed by interchanging variables in the EM equations. For example, specific energy E may be used as the state variable and time as the independent variable in one type of problem, but in another, it may be convenient to divide Eq. (78) by Eq. (83) to change the independent variable from time to mass.

- EM approximations generally treat either h or V as the control variable, since the dynamics of these quantities are neglected and the derivatives of the states ($\dot{E}$,$\dot{m}$,etc.) can be expressed in terms of these variables. V and h can be related to one another and to the state E by Eq. (79).

- In the context of an optimal control problem, the energy-state approximations imply that the control variable h or V varies slowly over most of the trajectory, but it may contain discontinuities and rapid variations confined to narrow regions. Various extensions to the EM methodology have been developed, for example by using singular perturbation theory to provide corrections to the approximate solution through analysis of the h and V dynamics in a "stretched" time scale [19] (see Section II).

(1) Minimum Time to Climb

Perhaps the most easily discernible application of EM methods is determining the altitude/velocity profile which minimizes the time to climb to a specified energy level. Minimizing the time to change energy levels is equivalent to maximizing the rate of change of energy $\dot{E}$ (Eq. (78)). Thus, the approximately optimal reference velocity (V_R) profile is the one which maximizes $\dot{E}$ for a given E, or mathematically:

$$V_R = \arg \max_V \{[(T(E,V)-D(E,V))V/m]\} \qquad (84)$$

which can be read "V_R is the value of V which maximizes the expression [(T-D)V/m] with respect to V."

When this expression (Eq. (84)) for the approximately optimal control is evaluated numerically, a solution path similar to that shown in Figure 22 typically results. The path is characterized by portions which satisfy Eq. (84), connected by portions of constant energy contours. Thus, the approximately minimum-time path from point A´ on energy level E_1 to point G on energy level E_2 is given by:

- a rapid dive to B´
- motion along the optimal segment B´C to point C
- a rapid dive to D*
- motion along the optimal segment DF to F
- a rapid climb (zoom) to G.

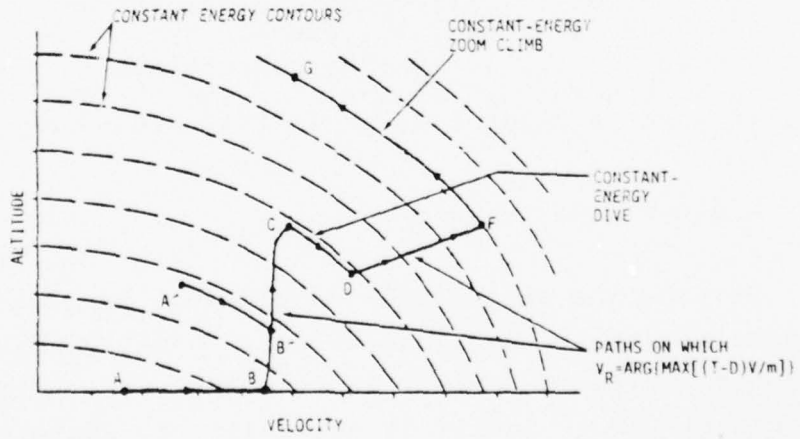


Figure 22. Typical Minimum-Time Climb Path to Higher Energy Level [18]

*This rapid dive is characteristic of transonic trajectories, where for certain aircraft it becomes more economical to gain velocity very quickly (by diving) so as to get through Mach 1 as rapidly as possible.

As shown in the figure, the approximately optimal path as derived from EM methods exhibits discontinuities in the control variable V, which appear as corners in the profile. These discontinuities stem from the energy state approximation, which neglects the dynamics of V and assumes that V and h can be traded instantaneously at constant energy levels using the relation:

$$h = (E - 1/2\ V^2)\ /g \tag{85}$$

More accurate solutions (four-dimensional state, numerical solution by the gradient method) do not exhibit such discontinuities (Figure 23), although overall agreement is good between the more accurate method and the much easier approximate EM method. A singular perturbation approach has been used [19] to analyze the discontinuities of the approximate method and compute corrections which effectively smooth the corners in the approximate solution.

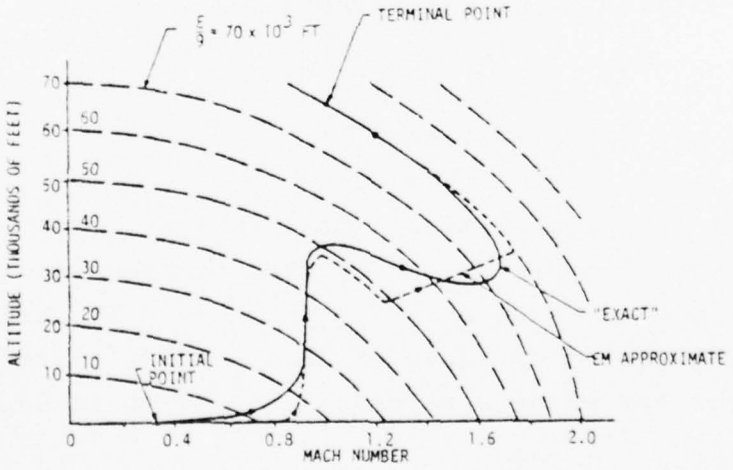


Figure 23. Comparison of "Exact" and Energy-State Minimum Time-to-Climb Paths [18]

The reference quantities generated by the minimum time-to-climb solution, then, are reference velocity V_R and reference altitude h_R. While these quantities are considered "controls" by the outer-loop solution, they are nevertheless states of the overall path control problem. Calculation of the remaining reference states and reference controls from these key reference quantities is discussed in Paragraph C below.

(2) Minimum Fuel Problems

Application of EM methods to minimum fuel problems often involves a change of independent variable from time to mass. This is done by dividing Eq. (83) into Eq. (78):

$$\frac{dE}{dm} = \frac{V(T-D)}{mf} \tag{86}$$

Minimizing the fuel used to change energy levels is equivalent to maximizing dE/dm, the rate of energy gain per change in mass. Thus, the approximately optimal reference velocity for fuel-minimum climb is:

$$V_R = \arg \left\{ \max_V \left[(T-D)V/mf \right] \right\} \tag{87}$$

An example [25] approximately minimum-fuel climb path is shown in Figure 24. For comparison, a standard recommended economical climb path (an 0.75 Mach climb) is also shown. The near optimal method saves 289 pounds of fuel, or 15.5 percent of the nominal expenditure, for the example aircraft in a climb to 30,000 feet.

(3) Maximum Range Problems

Application of EM methods to maximum range problems typically involves a change of independent variable from time to range coordinate. This is done by dividing Eq. (82) into Eq. (78) and Eq. (83):

$$\frac{dE}{dx} = (T-D)/m \tag{88}$$

$$\frac{dm}{dx} = f/V \tag{89}$$

To find the trajectory which minimizes fuel over a specified range $[x_o, x_f]$, one can minimize the total mass change subject to the energy state constraint; i.e., the cost function is:

$$J = \int_{x_o}^{x_f} \left(\frac{f}{V} + \lambda\ (T-D)/m\right)\ dx \tag{90}$$

Thus the approximately optimal reference velocity is given by:

$$V_R = \arg\ \{\min_V [\frac{f}{V} + \lambda\ (T-D)/m]\} \tag{91}$$

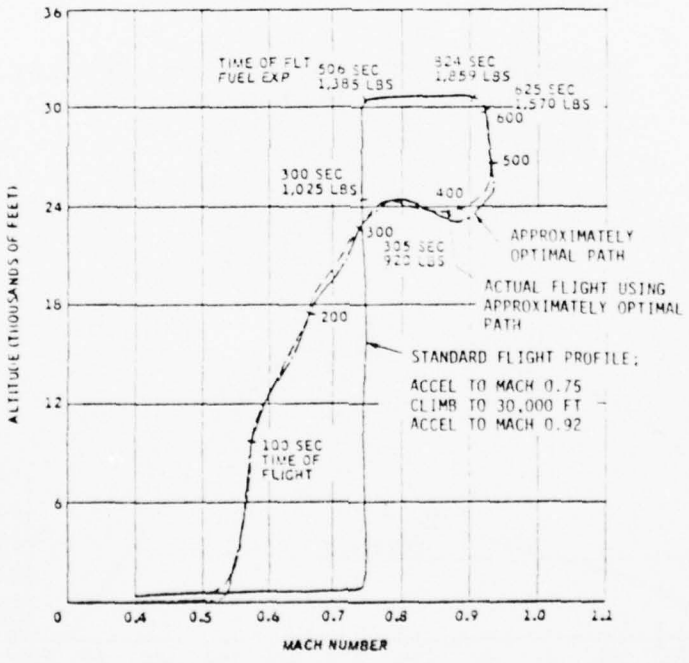


Figure 24. Comparison of Minimum-Fuel Climbs Using Standard Flight Profile and Approximately Optimal Path at Military Thrust [25]

Figure 25 shows a typical altitude/velocity profile for an approximately minimum-fuel climb, cruise, and descent to zero altitude at a specified range. Figure 26 presents corresponding plots of altitude and fuel versus range [25].

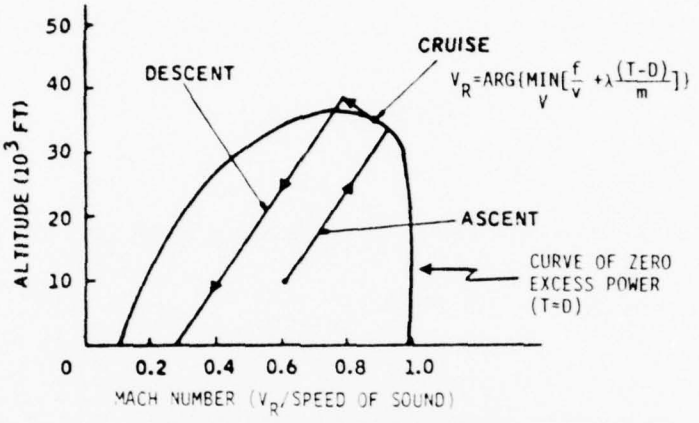


Figure 25. Minimum-Fuel Climb, Cruise, Descent - Altitude versus Mach Number

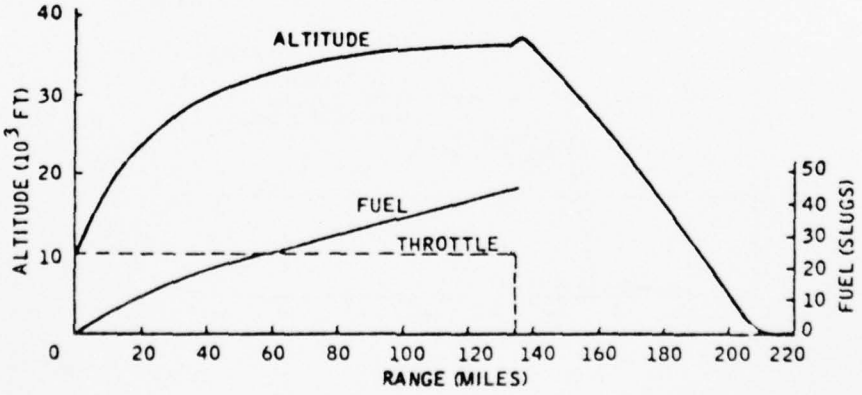


Figure 26. Minimum-Fuel Climb, Cruise, Descent - Altitude and Fuel versus Range

(4) Minimum Direct Operating Costs

Instead of minimizing the fuel usage alone over a fixed range, it may be more desirable to minimize a combination of fuel and transit time, expressed in terms of direct operating costs. Thus, the cost function to be minimized is:

$$J = c_f m_f + c_t(t_f - t_o) \tag{92}$$

where c_f and c_t are the unit costs of fuel and time, respectively, m_f is the mass of fuel burned, and $(t_f - t_o)$ is the transit time. In integral form, the cost can be written:

$$J = \int_{t_o}^{t_f} (f\, c_f + c_t)\, dt \tag{93}$$

where f is the fuel burn rate.

Solution for the altitude/range profiles which minimize direct operating costs (Eq. (93)) subject to the approximate state dynamics (Eqs. (78) through (83)) can now be addressed using the minimum principle. Typically, a change of variable as exemplified by Eqs. (88) through (90) is again used. Reference [30] presents some results for subsonic turbofan aircraft with the restriction that the solution trajectory consist of three segments: a monotonic climb to cruise energy level, a segment of optimal subsonic cruise, and a monotonic descent to the final energy level.

(5) Terrain-Following Guidance

The primary objective of terrain-following guidance is to minimize exposure to the enemy by producing flight paths which lie as close to all terrain points as possible. To be practical, however, the terrain-following guidance should produce reference trajectories which can be followed extremely well by actual aircraft.

The terrain-following control systems that are currently on operational aircraft compute flight-path angle commands based on

a "critical" point on the terrain ahead of the aircraft. For different systems, the methods vary for determining which point is currently the most critical. Since it is the flight-path angle, or slope, that is directly controlled, the actual vehicle path is not tightly controlled. The path is the integral of the slope with respect to range; therefore, the height error is the integral of the total slope errors, which are due to both sensor errors and control system implementation errors [31]. Operational terrain-following systems also rely on manual throttle control or on auto-throttles which attempt to maintain nearly constant speed; neither of these methods provides efficient engine operation, in terms of both engine life and fuel consumption.

To overcome these difficulties, recent research has been directed toward total path control, as opposed to the single "critical" point techniques discussed above. Focusing on the total path also allows simultaneous consideration of secondary objectives, such as meeting checkpoint times (controlled time of arrival) or optimizing engine performance (engine life or fuel consumption).

One of the total path techniques is based on the cubic spline* reference path [32]. The concept is illustrated in Figure 27 (p. 82). As shown, the reference altitude h_R path is tangent to the minimum clearance curve, but must be above it when the curvature of the terrain (and hence the clearance curve) is sufficiently sharp as to exceed the acceleration capability of the aircraft. The total solution path is formed by parametrically optimizing the cubic spline form subject to the operational constraints (g-limits, etc.) imposed. Using the differentiability property of the cubic spline, the optimization procedure can generate not only the reference altitude profile h_R but also the rates of change

---

* A cubic spline is a continuous curve consisting of cubic polynomial segments pieced together such that the curve has continuous first and second derivatives.

$\dot{h}_R$ and $\ddot{h}_R$. These, in turn, can be used to establish a complete and consistent set of reference states; for example, γ_R can be found from $\dot{h}_R$ by the relation:

$$\dot{h}_R = V_R \sin \gamma_R \tag{94}$$

once the reference velocity V_R is established.

Reference velocity can be determined so as to satisfy any of the secondary guidance objectives cited above. For example, the velocity which corresponds to sustained flight at a desired, allowable energy level may be selected as reference. Such an example is illustrated by Figure 28, which shows the given potential energy (gh_R) and the minimum and maximum total energy (potential plus kinetic) corresponding to sustained flight at the minimum and maximum allowable velocities (V_{min} and V_{max}). The figure illustrates allowable constant energy levels; i.e., those which lie totally within the allowable corridor over a reasonable range. Any of these allowable energy levels could be selected as the reference (E_R), say, on the basis of fuel consumption, engine life, mission timing, etc. The corresponding reference velocity is then found from:

$$V_R = \sqrt{2\ (E_R - gh_R)} \tag{95}$$

c. Calculation of Remaining Reference Quantities

The preceding has presented several guidance techniques which can be used to determine optimal reference values of selected state variables. The path-control concept, however, requires reference values for all states and controls considered. The calculation of the remaining reference states and nominal controls is not a trivial matter, since all the reference quantities must be mutually consistent if the overall design is to approach optimality. A very simple example of calculating such a "residual" reference state is by using the expression for heading rate during a coordinated turn:

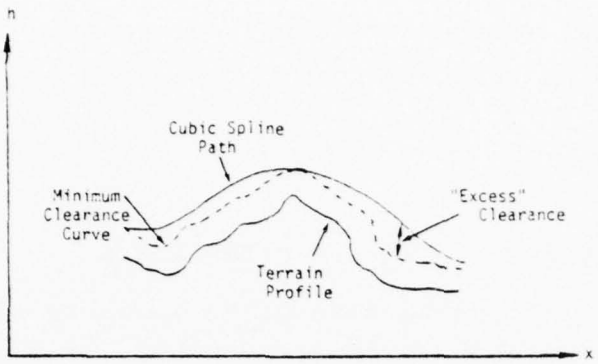


Figure 27. Cubic Spline Reference Path [32]

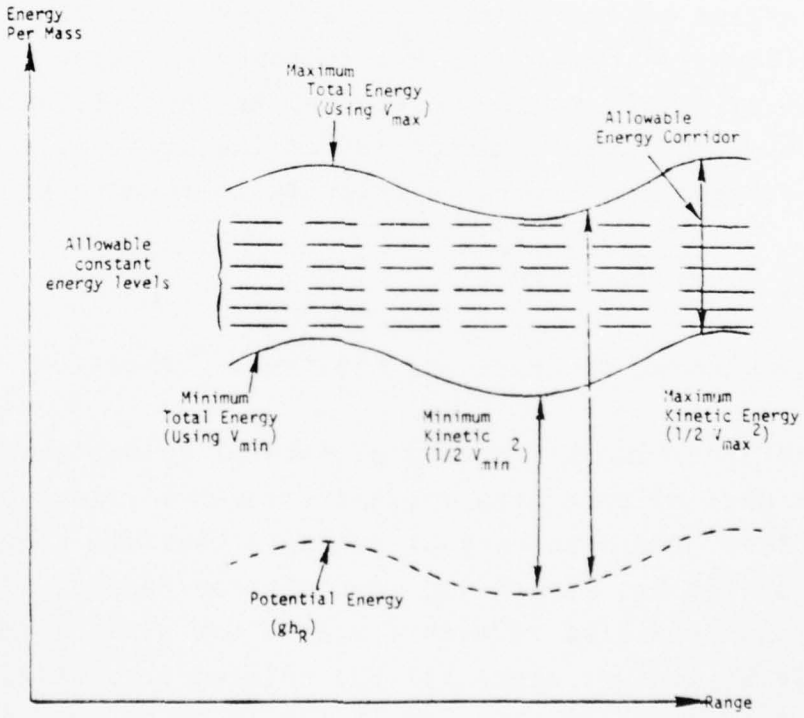


Figure 28. Energy Constraints Used to Determine V_R

$$\dot{\psi}_R = \frac{g}{V_R} \tan \phi_R \qquad (96)$$

Thus, given the reference bank angle ϕ_R, the consistent reference heading rate $\dot{\psi}_R$ is given approximately by Eq. (96).

More frequently, however, the designer must revert to a detailed, six degree of freedom nonlinear model of the aircraft (see Appendix) in order to generate a complete and consistent set of references. Frequently, iterative solutions of these nonlinear differential equations are required, or approximation techniques are used to reduce computational burden. Further discussion of such techniques is beyond the scope of this report.

4. PERTURBATION CONTROL

In the context of the path control problem, the primary objective of the perturbation control function is the accurate and efficient tracking of the reference state. Accurate tracking, or "departure prevention", serves to enhance the effectiveness of the reference generation function in achieving over-all path- control objectives. Constraining the departure from the reference has the added benefit that, by so doing, the linearity assumptions upon which the perturbation feedback controller design is based are indeed valid. Secondary objectives of the perturbation control function are <u>disturbance rejection</u>, <u>robustness</u> (i.e., the reduction in sensitivity to uncertainty in the controller design parameters), and <u>stability augmentation</u>.

The methods used to achieve these objectives are many and varied. Historically, classical frequency-domain techniques have been used to design simple analog or digital control loops to address the objectives on an individual basis. As air vehicles have increased in complexity (e.g., additional, redundant actuators) and mission objectives have increased in sophistication (e.g., path control), classical methods have given way to proven multivariable techniques for linear system design. Often, a design is formulated

using the more comprehensive (and direct) linear multivariable techniques and checked at various operating points or flight conditions using a classical analysis.

For illustration, two perturbation controller design examples are presented below, each utilizes a different design concept.

a. Lateral-axis Perturbation Control Design by Pole Placement Methods

For simplified motion in the lateral plane, only five states need be considered. These states, expressed in terms of their reference values and perturbation values, are:

$$\begin{aligned} x &= x_R + \delta x \\ y &= y_R + \delta y \\ \psi &= \psi_R + \delta\psi \\ V &= V_R + \delta V \\ \phi &= \phi_R + \delta\phi \end{aligned} \tag{97}$$

The reference values and their rates of change (if needed) are assumed to have been computed by the reference generator.

The objective is to obtain a closed-loop control system which will keep the perturbation values small. A classical pole-placement technique will be used for this example.

The first step in the technique [27] is to derive an adequate linear model of the aircraft state perturbation dynamics. The derivation begins with a highly simplified nonlinear model:

$$\begin{aligned} \dot{x} &= V \cos\psi \\ \dot{y} &= V \sin\psi \\ \dot{\psi} &= (g/V) \tan\phi \end{aligned} \tag{98}$$

Next, first-order variations are taken on Eq. (98) about the reference state:

$$\begin{aligned}
\delta\dot{x} &= -V_R \sin \psi_R \delta\psi + \cos \psi_R \delta V \\
\delta\dot{y} &= V_R \cos \psi_R \delta\psi + \sin \psi_R \delta V \\
\delta\dot{\psi} &= (g/V_R) \sec^2\phi \, \delta\phi - (\dot{\psi}_R/V_R)\delta V
\end{aligned} \tag{99}$$

To eliminate the $\sin \psi_R$ and $\cos \psi_R$ terms, Eq. (99) is rotated into the "moving target coordinate system" by the rotation:

$$\begin{bmatrix} \delta x' \\ \delta y' \end{bmatrix} = \begin{bmatrix} \cos \psi_R & \sin \psi_R \\ -\sin \psi_R & \cos \psi_R \end{bmatrix} \begin{bmatrix} \delta x \\ \delta y \end{bmatrix} \tag{100}$$

As shown in Figure 29, this coordinate system is attached to the reference or "phantom" position and oriented along the reference direction of travel.

The linear perturbation model in the moving target coordinate system, then, is:

$$\delta\dot{x}' = \delta V + \dot{\psi}_R \delta y' \tag{101}$$

$$\delta\dot{y}' = V_R \delta\psi - \dot{\psi}_R \delta x' \tag{102}$$

$$\delta\dot{\psi} = (g/V_R) \sec^2\phi_R \delta\phi - (\dot{\psi}_R/V_R) \delta V \tag{103}$$

As noted in Eqs. (101) and (102), the linearized equations are coupled through the reference heading rate $\dot{\psi}_R$, which, along with V_R and ϕ_R, is a parameter of the model.

Choosing bank angle and velocity magnitude as the control variables and using an empirically derived model of the aircraft/stability augmentation system, an over-all perturbation feedback

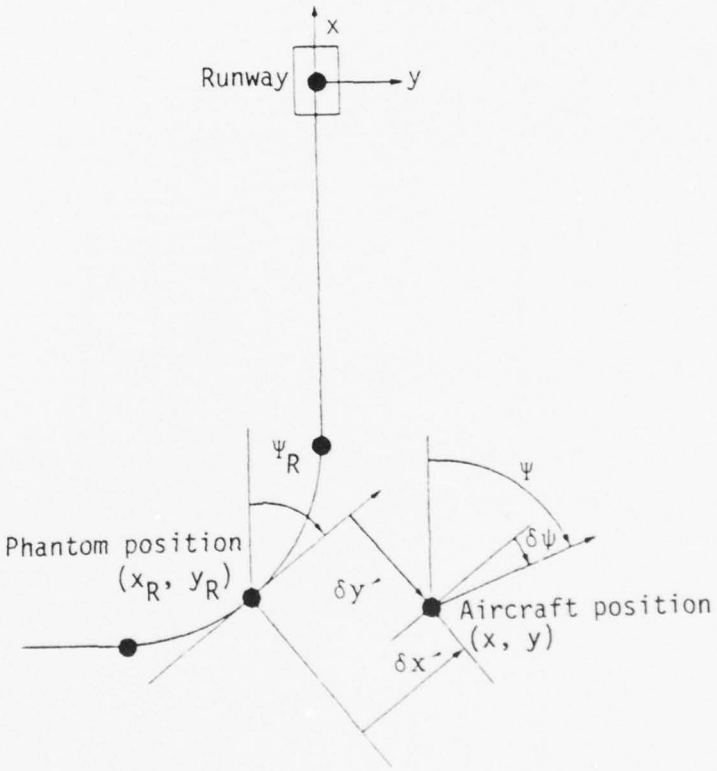


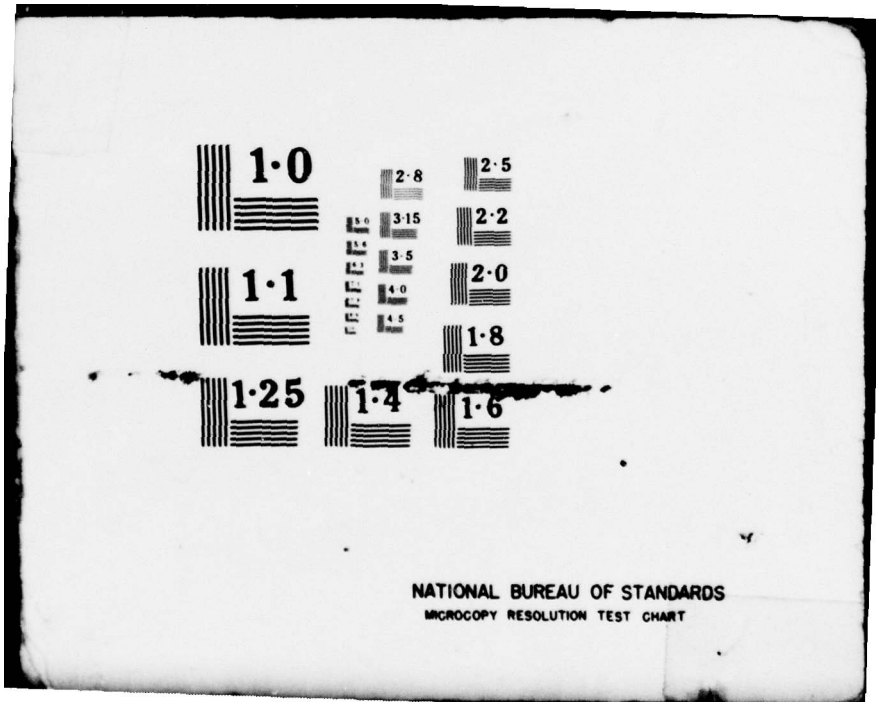
Figure 29. Moving Target Coordinate System [27]

AD-A070 252 SYSTEMS CONTROL INC PALO ALTO CALIF F/G 1/3
PATH CONTROLLERS: UNIFICATION OF CONCEPTS AND COMPARISON OF DES--ETC(U)
DEC 78 J E JONES, J S KARMARKAR F33615-77-C-3079
UNCLASSIFIED AFFDL-TR-78-178 NL

2 OF 2
AD
A070252



END
DATE
FILMED
7-79
DDC


1·0
1·1
1·25
2·8
3·15
3·5
4·0
4·5
2·5
2·2
2·0
1·8
1·4
1·6
NATIONAL BUREAU OF STANDARDS
MICROCOPY RESOLUTION TEST CHART

control system can be synthesized according to the structure shown in Figure 30. The perturbation control law can be expressed in the state feedback form:

$$\delta\phi_{fb} = -k_{\phi y}\delta y' - k_{\phi\psi}V_R\delta\psi + k_{\phi x}\dot{\Psi}_R\delta x' \tag{104}$$

$$\delta V_{fb} = -k_{vx}\delta x' - k_{vy}\dot{\Psi}_R\delta y' \tag{105}$$

The feedback gains are selected so as to achieve a desirable closed-loop configuration over a wide range of the parameters $\dot{\psi}_R$, V_R and ϕ_R. A preliminary eigenvalue analysis indicates that a reasonable response is achieved by using 0.000186 rad/ft for $k_{\phi y}$, 0.003863 rad/[rad (fps)] for $k_{\phi\Psi}$, 0.0001 rad/[ft (rad/sec)] for $k_{\phi x}$, 0.0444 (fps)/ft for k_{vx}, and 0.15 (fps)/[ft (rad/sec)] for K_{vy}. This combination of gain constants was obtained by trial and error using root-locus analysis of the system of equations. The eigenvalues corresponding to this set of gains yield reasonable frequency and damping. Figure 31 shows three branches of the root locus plot for this set of gains as a function of $\dot{\psi}_R$, ranging from 0°/sec to 6°/sec. The dashed and solid lines are root loci of a system with and without the cross feedback gains $k_{\phi x}$ and k_{vy}. At $\dot{\psi}_R$ = 0°/sec, the damping ratio for the upper and lower branches are 0.52 and 0.86 respectively. At $\dot{\psi}_R$ = 6°/sec, the damping ratio for the upper branch is 0.23 for a system with cross feedback and 0.15 for a system without cross feedback and for the lower branch, it is 0.82 for the system with cross feedback and 0.78 for the system without cross feedback. The root loci illustrate a definite improvement on system stability by using cross feedback.

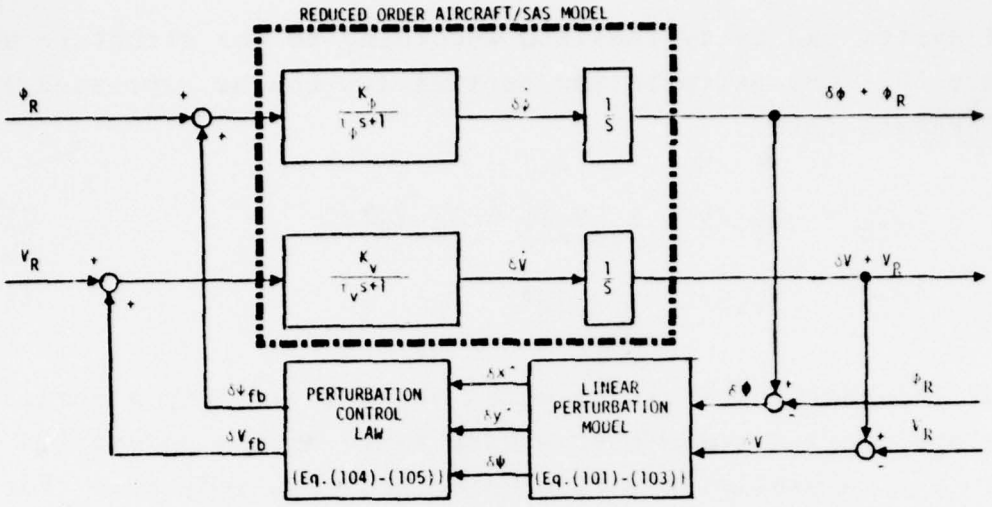


Figure 30. Structure of the Perturbation Feedback Control System

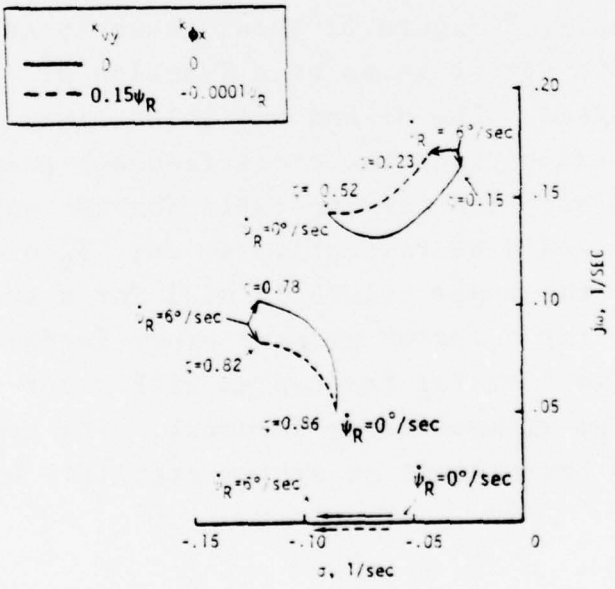


Figure 31. Root Locus of Closed-Loop Feedback Systems [27]

b. STOL Flare Autopilot Design by Quadratic Synthesis

Linear regulator theory (linear-quadratic design or quadratic synthesis) provides a basis for the design of controllers which follow a desired output state. While the usual quadratic synthesis procedure outlined in Section II may be adequate for minimizing the average departure from the reference, much tighter tracking of a particular reference state component (e.g., altitude profile) may be required. One way of providing this increased tracking capability is to put tracking error directly into the cost functional. In this way, the feedback gains derived from quadratic synthesis are exactly those which optimize tracking of the reference. Unfortunately, solution of the optimal linear tracking (or "servomechanism") problem involves the computation of an additional open-loop control term, the solution for which depends upon the entire desired profile. Thus the entire profile must be known a priori in order for the solution to be realizable. While this restriction is severely limiting, the tracking problem does have practical validity, as illustrated in this section for the example where a desired altitude profile is tracked during the aircraft flare maneuver.

The purpose of the flare maneuver is to reduce the aircraft rate of descent just prior to touchdown during landing. The touchdown should be made at a sink rate less than 2 ft/sec to meet structural and passenger comfort constraints. The nonzero sink rate is desired to decrease touchdown dispersion. The 2 ft/sec sink rate corresponds to a flight path angle of -0.5° for conventional takeoff and landing (CTOL) operations using an airspeed of 130 knots (230 ft/sec); it corresponds to about -1.0° for short takeoff and landing (STOL) operations using an airspeed of 65 knots (110 ft/sec). The flare maneuver is necessary because the approach to the runway must be made at a considerably steeper flight path angle than is acceptable for touchdown. Steeper flight path angles reduce ground noise near the airport, avoid obstacles, and make the touchdown point more precise. Conventional aircraft

operations use a flight path angle of about -2.5% during approach; STOL operations use a flight path angle of about -7.5°. Figure 32 illustrates a typical flare maneuver for STOL aircraft.

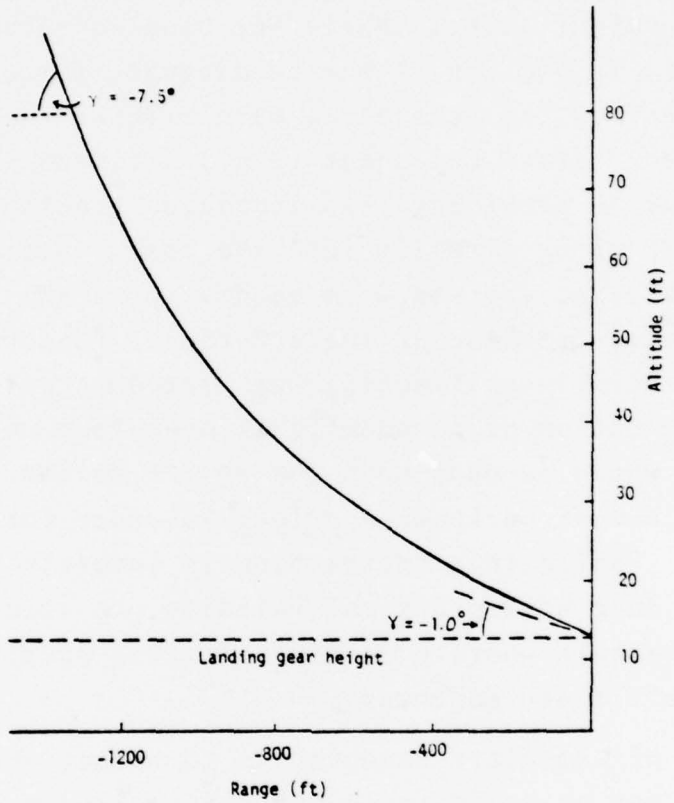


Figure 32. Typical STOL Flare Maneuver [33]

The flare autopilot must manage a number of state variables so as to effect a smooth glide-path transition, restrain terminal error to acceptable bounds, and obey constraints (e.g., maximum angle-of-attack or flap limits) along the path. Moreover, particularly for STOL vehicles, the autopilot can make use of a number of control effectors -- elevator, speed (thrust), nozzle deflection (for vector thrust vehicles), flap deflection, etc. Clearly, this is a problem well suited to multivariable design techniques, such as the linear-quadratic-optimal design (quadratic synthesis, see Section II).

As usual, the quadratic synthesis procedure begins with a linear model of the STOL aircraft. The state variables are again divided into reference and perturbation values.

$$
\begin{aligned}
V &= V_R + \delta V \\
\gamma &= \gamma_R + \delta\gamma \\
\theta &= \theta_R + \delta\theta \\
q &= 0 + \delta q \\
h &= h_R + \delta h
\end{aligned}
\tag{106}
$$

where

V is the velocity

γ is the flight path angle

θ is the pitch angle

q is the pitch rate

h is the altitude

The controls are

$$
\begin{aligned}
e &= e_R + \delta e \\
n &= n_R + \delta n \\
T &= T_R + \delta T \\
F &= F_R + 0
\end{aligned}
\tag{107}
$$

where

e is the elevator deflection

n is the nozzle deflection (thrust vector)

T is the thrust

F is the flap setting (fixed at the value F_R)

The linear perturbation equations with coefficients evaluated at the indicated reference conditions are shown in Figure 33; the selected STOL aircraft is the NASA Ames Augmentor Wing Jet STOL Research Aircraft (AWJSRA).

Key to the design is the definition of an appropriate desired altitude "error" profile* δh_D for the perturbation controller to follow. One reasonable choice [33] is simply an exponential fit through the initial altitude error δh_o and meeting a zero altitude terminal condition:

$$\delta h_D(t) = \delta h_o \exp(-t/\tau_h) \tag{108}$$

where the time constant parameter τ_h is defined so as to match end conditions.

The desired altitude error profile enters the controller design through the performance index, as follows:

$$J = \frac{1}{2}\delta\underline{x}^T S_f \delta\underline{x} + \frac{1}{2}\int_{t_o}^{t_f} \Big[\left(M\delta\underline{x} - \delta h_D(t)\right)^2 W_h + \delta\underline{u}^T W \delta\underline{u} \Big] dt \tag{109}$$

where S_f, W_h, and W_u are the usual penalty weights and M is the 1×5 matrix that picks out the altitude state error for comparison with δh_D:

$$M = [0\ 0\ 0\ 0\ 1] \tag{110}$$

---

*In other words, the desired altitude h_D is thought of as an "error" from the desired terminal condition $h(t_f) = 0$.

$$\delta\dot{\underline{x}} = F\delta\underline{x} + G\delta\underline{u}$$

where

$$\delta\underline{x} = \{\, \delta v \quad \delta\gamma \quad \delta\theta \quad \delta q \quad \delta h \,\}^T$$

$$\delta\underline{u} = \{\, \delta e \quad \delta n \quad \delta T \,\}^T$$

$$F = \begin{bmatrix} -0.0397 & -0.280 & -0.282 & -0.0027 & 0.0 \\ 0.135 & -0.538 & 0.538 & 0.0434 & 0.0 \\ 0.0 & 0.0 & 0.0 & 1.0 & 0.0 \\ 0.0207 & 0.441 & -0.441 & -1.41 & 0.0 \\ -0.017 & 1.92 & 0.0 & 0.0 & 0.0 \end{bmatrix}$$

$$G = \begin{bmatrix} -0.0052 & -0.102 & 0.21 \\ 0.031 & 0.037 & 0.35 \\ 0.0 & 0.0 & 0.0 \\ -1.46 & -0.066 & 0.15 \\ 0.0 & 0.0 & 0.0 \end{bmatrix}$$

Equilibrium Values	Trim Condition
V_R = 110 ft/sec	e_R = -9.6°
γ_R = -1.0°	n_R = 55.4°
θ_R = +1.3°	T_R = 24.0°
	F_R = 65.0°

Figure 33. Longitudinal Dynamics of Typical STOL Aircraft [33]

The performance index (Eq. (109)) penalizes along-path deviations from the desired altitude error profile. This is the tracking servomechanism problem of linear regulator theory (see Ref. 17, Section 5.2). The solution is, using the backward sweep method of Section II:

$$\delta \underline{u} = - W_u^{-1} G^T (S\delta \underline{x} + \underline{\xi}) \tag{111}$$

where S is the Riccati matrix, obtained by the solution to the Riccati Equation:

$$\dot{S} - -SF - F^T S + SGW_u^{-1} G^T S - M^T W_h M \tag{112}$$

and ξ is the vector of control driving terms*, which satisfy:

$$\dot{\underline{\xi}} = \left| -F^T + SGW^{-1} G^T \right| \underline{\xi} + M^T W_h \delta h_D \tag{113}$$

Numerical values were found in [33] for the time-varying feedback gains of Eq (111):

$$K_x = -W_u^{-1} G^T S \tag{114}$$

and the control driving terms $\underline{\xi}$. The numerical values correspond to the terminal and along-path weightings (i.e. square-root of the reciprocals of the diagonal elements of S_f, W_h, and W_u) as shown in Table 4. An altitude profile generated by the perturbation control law in a linear simulation is shown in Figure 34. As can be seen, the reference desired altitude profile is tracked very closely.

---

* Such an additional term appears in the solution to the regulator problem either when the regulator must track a desired output or when the plant is driven by a non-white noise or disturbance vector [17].

TABLE 4
TERMINAL AND ALONG-PATH WEIGHTINGS FOR FLARE AUTOPILOT DESIGN

Variable	Terminal Weight (i.e., max value)	Along-Path Weight (i.e., max value)
δv	5 ft/sec	-
$\delta \gamma$	1°	-
$\delta \theta$	3°	-
δq	1 °/sec	-
δh	2 ft	4 ft
δe	-	2°
δn	-	10°
δT	not used	not used

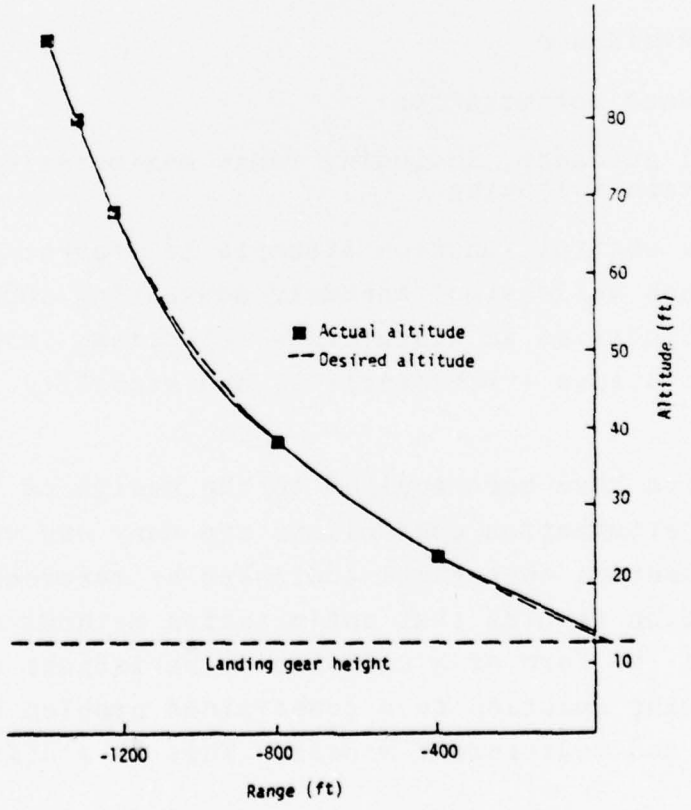


Figure 34. Altitude vs. Range from Linear Simulation Using Time-Varying Feedback Gain

SECTION IV
CONCLUSIONS AND RECOMMENDATIONS

1. CONCLUSIONS

The path-control framework has been shown to be a useful formal structure for addressing a large number of modern aircraft guidance and control problems. The structure has two main functional partitions: (1) a reference (trajectory) generator and (2) a perturbation controller. The reference generation partition encompasses such "outer loop" control functions as:

- horizontal guidance, including controlled time of arrival
- threat avoidance
- performance optimization
- vertical guidance, including range maximization and terrain following.

The perturbation control function attempts to prevent departures from the reference while simultaneously addressing such "inner loop" control objectives as disturbance rejection, insensitivity to parameter variations ("robustness"), and stability augmentation.

Methods which have been applied to the design of reference generators and perturbation controllers are many and varied. Typically, the control objectives addressed by reference (trajectory) generation require that optimization methods be applied. Often this takes the form of a calculus of variations or mathematical programming solution to a constrained problem with nonlinear state and measurement models. This is a difficult

and computational resource-consuming process; and modeling simplifications must be made and alternative computer architectures must be explored to implement such solutions in real time. For the perturbation control function, classical frequency-domain techniques have been used to design simple analog or digital control loops to address the objectives on an individual basis. As air vehicles have increased in complexity (e.g., additional, redundant actuators) and mission objectives have increased in sophistication (e.g., path control), classical methods have given way to proven multivariable techniques for linear system design. Often, a design is formulated using the more comprehensive (and direct) linear multivariable techniques and checked at various operating points or flight conditions using a classical analysis.

2. RECOMMENDED STUDY AREAS

Several topics addressed in this report present themselves as potentially high payoff areas for further research. In general, the previous work reported upon is theoretical in nature and has yet to be developed into working designs. Such development and implementation of existing theoretical concepts is a difficult and multifaceted problem, involving:

(1) thorough understanding of theoretical concepts so that any approximations or assumptions necessary to make the concept "implementable" can be assured to be valid; and

(2) broad expertise with state-of-the-art computing systems so that computational resources can be efficiently assigned to the appropriate processing task and so that the final design will be well integrated.

Because of the difficulties anticipated with bringing modern guidance and control concepts to an operational stage, it is

recommended that future research emphasize real-time laboratory evaluation and in-flight testing in the development and validation of such concepts. Particular recommended study topics are enumerated below.

a. Threat Avoidance

The Air Force Flight Dynamics Laboratory (FDL) is currently funding the development and demonstration of a 4-D Integrated Control and Display System (INCADS). The following advanced flight management capabilities are to be provided by the 4-D INCADS system:

- Airborne computer synthesis of nonlinear four-dimensional profiles (3D trajectories plus time)
- A control law (with automatic and manual modes) to track the synthesized 4-D profiles
- Mission-oriented information displays and controls

In addition to endpoint attainment, the 4-D profile synthesis capability is being used to avoid military threats, traffic, obstacles, and weather. Recent work has been directed towards transport aircraft; the emphasis is now shifting towards fighter aircraft.

As discussed in Section III, the state-of-the-art in practical control theory now permits much more comprehensive and accurate solutions to the threat avoidance problem. The advent of high-speed parallel processing computer systems has made feasible the onboard implementation of trajectory generation algorithms which simultaneously optimize:

- probability of survival for both completing and aborting the mission at a particular time
- probability of accomplishing numerous mission objectives (striking targets, etc.)

- strategy for deploying both expendable and non-expendable countermeasure resources.

Research on such advanced algorithms may prove to be of high potential payoff, particularly for the case of fighter aircraft on missions which require penetration of heavy defenses.

b. Terrain Following

Modern path-oriented approaches to the terrain-following problem offer many options to the system designer. These include:

- how to incorporate a priori and real-time-collected information about the terrain along the desired track
- what secondary performance objectives (fuel optimization, throttle activity optimization, etc.) should be addressed by the reference generation algorithms
- how to make these sophisticated solutions computable in real time.

Design techniques already exist for addressing the various aspects of the problem, but these have yet to be integrated into a working system. The design, development, and demonstration of such an integrated system are worthwhile research objectives.

c. Advanced Perturbation Control

Perturbation control, as presented in this report, is an integral part of the path-control problem as associated with any research performed on reference generation (e.g., the threat-avoidance and terrain-following work recommended above). Additionally, future work should be directed towards inner loop control itself, independent of reference generation. Such work

may address improved autopilot designs or the feasibility of active control concepts (ride smoothing, gust-load alleviation, etc.).

A prerequisite for such research is an accurate, high-fidelity mathematical model of the airframe aerodynamics, the actuation system, and the sensor system. These models must be tailored to the particular vehicle configuration and validated by test data. The reduction of test data and the development of the math models is greatly facilitated and semi-automated by the use of any of a number of parameter identification techniques, which basically attempt to select parameters in a prespecified model structure such that the model outputs "fit" the test data in some statistically optimal sense (e.g., maximum likelihood). Current FDL plans for instrumenting the KC-135C aircraft (Speckled Trout) are consistent with the information requirements of advanced parameter identification techniques. In view of the importance of this aircraft to FDL research and development efforts, it is recommended that advanced identification techniques in fact be applied to Speckled Trout flight data, in order to obtain a validated math model of sufficient fidelity to support all anticipated research activities.

APPENDIX
MODELING OF AIRCRAFT SYSTEMS FOR CONTROL DESIGN

A.1 INTRODUCTION

Mathematical models have been applied widely to the design of aerospace vehicle control systems. Such models vary broadly according to the nature of the particular physical process (aerodynamics, airframe bending, navigation and guidance, etc.) and the specific fidelity requirements imposed on the model by the system design objectives. This appendix highlights a few of the many modeling and approximation techniques which are normally applied to the design of aircraft guidance and control systems.

A.2 SIX-DEGREE-OF-FREEDOM (6 DOF) AIRCRAFT MODELS

While simple point mass models are sufficient for many aircraft performance prediction problems, inner loop design (e.g., the design of active controls) requires the fidelity of a full 6 DOF aircraft model. This section summarizes some of the results derived in [4], Chapters 5 and 6. For a more thorough treatment, the reader is referred to that work.

The general 6 DOF equations of motion for a rigid body derive from Newton's Law and the moment equation:

$$\underline{F} = \frac{d}{dt}(m\underline{v}) \tag{A.1}$$

$$\underline{G} = \frac{d\underline{h}}{dt} \tag{A.2}$$

where $\underline{F}$ resultant external force vector acting on the center of mass

$\underline{G}$ resultant external moment vector acting about the center of mass

$\underline{v}$ velocity vector of the center of mass

$\underline{h}$ angular momentum vector

m mass

In the above equations, the derivative is taken in the space-fixed (inertial) coordinate frame. Transforming these equations from the inertial frame to one rotating with a rate and rotation axis given by $\underline{\omega}$ and attached to the body, one obtains

$$\underline{F} = m \frac{\delta \underline{v}}{\delta t} + m(\underline{\omega} \times \underline{v}) \tag{A.3}$$

$$\underline{G} = \frac{\delta \underline{h}}{\delta t} + \underline{\omega} \times \underline{h} \tag{A.4}$$

where the derivative $(\delta/\delta t)$ is now taken in the rotating body frame.

The external force vector $\underline{F}$ is the sum of two components, the aerodynamic forces (including propulsive terms) $\underline{F}_A$ and a gravity term $\underline{F}_G$:

$$\underline{F} = \underline{F}_A + \underline{F}_G \tag{A.5}$$

In conventional aircraft body coordinates, these vectors have the components:

$$\underline{F}_A = \begin{bmatrix} X \\ Y \\ Z \end{bmatrix} \tag{A.6}$$

$$\underline{F}_G = \begin{bmatrix} -\, m\, g\, \sin\theta \\ +\, m\, g\, \cos\theta\, \sin\phi \\ +\, m\, g\, \cos\theta\, \cos\phi \end{bmatrix} \tag{A.7}$$

where θ is the body pitch angle

ϕ is the body roll angle

g is the acceleration of gravity

and the Euler angle sequence from inertial to body coordinates is assumed to be yaw-pitch-roll $\{\psi,\theta,\phi\}$. Letting the components of the velocity vector be, in body coordinates:

$$\underline{v} = \begin{bmatrix} u \\ v \\ \omega \end{bmatrix} \tag{A.8}$$

and letting the rotation rate of the body with respect to earth-fixed coordinates be, in body coordinates:

$$\underline{\omega} = \begin{bmatrix} p \\ q \\ r \end{bmatrix} \tag{A.9}$$

and letting the rotation rate of the earth with respect to inertial (space-fixed) coordinates be

$$\underline{\omega}^E = \begin{bmatrix} p^E \\ q^E \\ r^E \end{bmatrix} \tag{A.10}$$

one can write the force equilibrium equation (A.3) in component form:

$$\begin{aligned} X - mg\sin\theta &= m\left[\dot{u} + (q^E+q)w - (r^E+r)v\right] \\ Y + mg\cos\theta\sin\phi &= m\left[\dot{v} + (r^E+r)u - (p^E+p)w\right] \\ Z + mg\cos\theta\cos\phi &= m\left[\dot{w} + (p^E+p)v - (q^E+q)u\right] \end{aligned} \tag{A.11}$$

Equations (A.11) can be simplified by means of the <u>flat-earth approximation</u>, where $\underline{\omega}^E$ is neglected and the Earth is treated as a stationary plane in inertial space. In this case, the terms p^E, q^E and r^E disappear from the equations.

Similarly, one can write the moment equation in component form:

$$L = I_x\dot{p} - I_{yz}(q^2-r^2) - I_{zx}(\dot{r}+pq) - I_{xy}(\dot{q}-rp) - (I_y-I_z)qr$$

$$M = I_y\dot{q} - I_{zx}(r^2-p^2) - I_{xy}(\dot{p}+qr) - I_{yz}(\dot{r}-pq) - (I_z-I_x)rp$$

$$N = I_z\dot{r} - I_{xy}(p^2-q^2) - I_{yz}(\dot{q}+rp) - I_{zx}(\dot{p}-qr) - (I_x-I_y)pq \quad (A.12)$$

where the external moment vector has been expressed in its body axis components:

$$\underline{G} = \begin{bmatrix} L \\ M \\ N \end{bmatrix} \quad (A.13)$$

and the angular momentum components and their derivatives have been expressed in terms of the moments of inertia I_{ij}. The moment equation (A.12) has been reduced in complexity by the assumption that "mean"* inertia axes are used, that the inertia matrix is constant (e.g., fuel consumption has a negligible effect on inertia), and rotor effects (e.g., propeller) are negligible. If the X-Z plane is a plane of symmetry, as is usually the case for flight vehicles, $I_{xy} = I_{yz} = 0$ and Equations (A.12) reduce further:

$$L = I_x\dot{p} - I_{zx}(\dot{r}+pq) - (I_y-I_z)qr$$

$$M = I_y\dot{q} - I_{zx}(r^2-p^2) - (I_z-I_x)rp$$

$$N = I_z\dot{r} - I_{zx}(\dot{p}-qr) - (I_x-I_y)pq \quad (A.14)$$

---

* Mean axes are those body axes for which the angular momentum vector is not affected by distortion effects, such as elastic deformation, the motion of hinged parts, or the sloshing of fuel.

Using the flat-earth approximation, Eqs. (A.11) and (A.14) can be written in the state-space structure:

$$\dot{u} = \frac{1}{m}\left[X - m\,g\,\sin\theta + r\,v - q\,w\right]$$

$$\dot{v} = \frac{1}{m}\left[Y + m\,g\,\cos\theta\,\sin\phi + p\,w - r\,u\right]$$

$$\dot{w} = \frac{1}{m}\left[Z + m\,g\,\cos\theta\,\cos\phi + q\,u - p\,v\right]$$

$$\dot{p} = \left[L - qr(I_z - I_y) + I_{xz}pq + \left\{N - pq(I_y - I_x) - I_{xz}\,qr\right\} \cdot \frac{I_{xz}}{Iz}\right] \Big/ \left(I_x - \frac{I_{xz}^2}{Iz}\right)$$

$$\dot{q} = \frac{M}{I_y} + (r^2 - p^2)\,\frac{I_{xz}}{I_y} - pr\,\frac{(I_x - I_z)}{I_y}$$

$$\dot{r} = \left[N - pq(I_y - I_x) - I_{xz}qr + \left\{L + qr(I_y - I_z) + I_{xz}\,pq\right\} \cdot \frac{I_{xz}}{I_x}\right] \Big/ \left(I_z + \frac{I_{xz}^2}{I_x}\right) \qquad \text{(A.15)}$$

These six equations can be expressed in vector form:

$$\dot{\underline{x}} = \underline{f}(\underline{x}, \underline{F}, \underline{G}) \qquad \text{(A.16)}$$

by defining the state vector:

$$\underline{x} = \begin{bmatrix} u \\ v \\ w \\ p \\ q \\ r \end{bmatrix} \qquad \text{(A.17)}$$

Linear Model

For many reasons, it is common practice to "linearize" Equation (A.16) by assuming equilibrium (trim) conditions exist and examing small disturbances (perturbations) about this equilibrium. The application of this small disturbance theory leads to the general, coupled, linearized model of aircraft motion referred to steady-state, rectilinear flight. In the linearized equations, the components of the external forces $\underline{F}$ and moments $\underline{G}$ are "expanded" into linear expressions in the state perturbation variables; the coefficients of the linear expansion are the "stability derivatives."

These linearized equations are then usually "decoupled" into longitudinal and lateral axes by making several assumptions. The existence of "pure" (uncoupled) longitudinal motion depends on only three assumptions (in addition to the linearization assumptions):

(1) The flat-earth approximation

(2) The existence of a plane of symmetry

(3) The absence of rotor gyroscopic effects

The existence of the uncoupled lateral motions, however, depends upon more restrictive conditions; namely, those above plus the neglect of all aerodynamic cross-coupling terms (which may not be strictly zero).

The resulting linear equation in parametric form will not be reiterated here. For detailed development, the reader is referred to Ref. 4, Section 5.10 and following, or to another flight dynamics book.

A.3 POINT-MASS AIRCRAFT MODELS

Point mass aircraft models are highly desirable for designing outer-loop control laws (navigation/guidance, trajectory generation) because of their simplicity. Point-mass models are also used extensively in aircraft design to predict performance capabilities. Such models are based on force and moment equilibrium, geometry, and basic aerodynamics.

For illustration, the point mass model for aircraft motion in the vertical plane will be presented. Figure A.1 shows the nomenclature commonly used for this vertical-plane, point-mass model. As shown, the "wind-axis" (w) system is being used as reference; wind axes are defined by the x-axis into the relative wind and the z-axis opposing the lift vector.

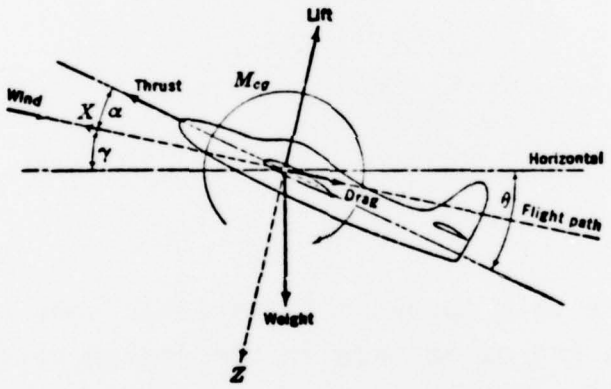


Figure A.1 Forces in the Aircraft Plane of Symmetry

In the rotating wind-axis coordinate frame, the x and z acceleration components are given by (assuming stationary atmosphere):

$$a_x^w = \dot{V} \tag{A.18}$$

$$a_z^w = V\dot{\gamma} \tag{A.19}$$

where V is the magnitude of the velocity relative to the air and γ is the flight path angle. Force equilibrium, then, leads to the following:

$$m\dot{V} = T\cos\alpha - D - mg\sin\gamma \tag{A.20}$$

$$mV\dot{\gamma} = T\sin\alpha + L - mg\cos\gamma \tag{A.21}$$

and the position equations can be written from geometry:

$$\dot{h} = V\sin\gamma \tag{A.22}$$

$$\dot{x} = V\cos\gamma \tag{A.23}$$

In the above equations, α is the angle-of-attack, T is the thrust, L is the lift, and D is the drag. Equations (A.20) (A.23) can be written in state space form by defining the state vector:

$$\underline{x} = \begin{bmatrix} x \\ h \\ V \\ \gamma \end{bmatrix} \tag{A.24}$$

The remainder of this Appendix illustrates some additional approximations which are often made in the design of control systems to maximize performance.

Quasi-Steady Approximation

Performance analysis of subsonic aircraft can frequently utilize the quasi-steady approximation, where accelerations are neglected in Equations (A.20) and (A.21), which become:

$$0 = T(V,h)\cos\alpha - D(\alpha,V,h) - mg\sin\gamma \tag{A.25}$$

$$0 = T(V,h)\sin\alpha + L(\alpha,V,h) - mg\cos\gamma \tag{A.26}$$

Now, for example, to determine the value of α^* which maximizes the rate of climb at a given altitude, one optimizes the expression for rate of climb (Eq. (A.22)):

$$\dot{h} = \text{rate-of-climb} = V \sin\gamma \tag{A.27}$$

subject to the constaints given by (A.25) and (A.26). That is, one finds the value of α which optimizes the Hamiltonian H :

$$H = V \sin\gamma + \lambda_1(T \cos\alpha - D - mg \sin\alpha) + \lambda_2(T \sin\alpha + L - mg \cos\alpha) \tag{A.28}$$

where λ_1, λ_2 are the lagrange multipliers (see Section 2.3.1).

Energy State Approximation

The energy state approximation [18] replaces $\dot{V}$ in Eq. (A.20) by energy per unit mass E as a state variable, where E is the sum of kinetic and potential energy:

$$E = 1/2\ V^2 + gh \tag{A.29}$$

The time rate of change of E is found by differentiating:

$$\dot{E} = V\dot{V} + g\dot{h} \tag{A.30}$$

and using Equation (A.20) to eliminate $\dot{V}$ and Equation (A.22) to eliminate $\dot{h}$:

$$\dot{E} = V\ (T\cos\alpha - D)/m \tag{A.31}$$

The approximation goes on to make the following additional assumptions:

---

*i.e., α is being used as a control variable in this outer-loop problem

(1) acceleration normal to the flight path ($V\dot{\gamma}$) is neglected;

(2) flight is nearly horizontal ($\cos\gamma \simeq 1$);

(3) the component of thrust normal to the flight path ($T \sin\alpha$) is neglected and $\cos\alpha \simeq 1$.

With these assumptions, Equation (A.21) reduces to:

$$L(\alpha,V,h) \simeq mg \tag{A.32}$$

which may then be used to determine α in terms of V and h :

$$\alpha = \alpha(V,h) \tag{A.33}$$

The altitude h may also be expressed in terms of V and the state E using Equation (A.29):

$$h = (E - 1/2\ V^2)/g \tag{A.34}$$

This permits final summary of the <u>energy state approximation</u>:

Using the energy state approximation, performance optimization may be addressed by considering a single state variable:

$$\dot{E} = V(T-D)/m \tag{A.35}$$

and V may be considered as the control variable, because both α and h can be expressed as a function of V (Equations (A.33) and (A.34)).

REFERENCES

1. Meyer, G. and Cicolani, L., "A Formal Structure for Advanced Automatic Flight Control Systems," NASA TN D-7940, May 1975.

2. Bird, D. and Neighbor, T. (Air Force Flight Dynamics Laboratory) – "Decoupling Control Technology for Medium STOL Transports," NASA TM X-3409, August 1976.

3. Vincent, James H., "STOL Tactical Aircraft Investigation – Flight Control Technology: Piloted Simulation of a Medium STOL Transport with Vectored Thrust/Mechanical Flaps," AFFDL-TR-73-19, Volume V, Part II, May 1973.

4. Etkin, B., Dynamics of Atmospheric Flight, John Wiley and Sons, 1972.

5. Athans, M., "The Role and Use of the Stochastic Linear-Quadratic-Gaussian Problem in Control System Design," IEEE Transactions on Automatic Control: Special Issue on the Linear-Quadratic-Gaussian Problem, Vol. AC-16, No. 6, December 1971.

6. Athans, M. and Falb, P., Optimal Control: An Introduction to the Theory and Its Applications, McGraw-Hill Book Company, New York, 1966.

7. Kokotovic, P., O'Malley, R., and Sannuti, P., "Singular Perturbations and Order Reduction in Control Theory -- An Overview," Automatica, Vol. 12, pp. 123-132, Reprint 1976 by Permagon Press, Great Britain.

8. Calise, A., "Singular Perturbation Methods for Variational Problems in Aircraft Flight," IEEE Transactions on Automatic Control, Vol. AC-21, No. 3, June 1976, pp. 345-353.

9. Davison, E., "A Method for Simplifying Linear Dynamic Systems," IEEE Transactions on Automatic Control, Vol. AC-11, pp. 93-100, 1966.

10. De Hoff, R., Hall, W.E., Adams, R., and Gupta, N., "F100 Multivariable Control Synthesis Program -- Vol. 1 Design Methodology," Systems Control, Inc. (Vt) Report to AFAPL under Contract F33615-75-C-2053, January 1977.

11. Rogers, R. and Sworder, D., "Suboptimal Control of Linear Systems Derived from Models of Lower Dimension," AIAA Journal, August 1971, pp. 1461-1467.

12. Skelton, R., "Cost-sensitive Model Reduction for Control Design," AIAA Paper 78-1282, Guidance and Control Conference, Palo Alto, CA, August 1978.

13. van Woerkom, P.Th.L.M., "Survey of Modern Control and Observation Theory for Disturbed, Target Following Aerospace Systems," National Aerospace Laboratory, The Netherlands, Report NLR-TR-76041-U, March 1976.

14. Bryson, A. and Ho, Y.C., Applied Optimal Control, Blaisdell Publishing Co., Waltham, Mass., 1969.

15. Pontryagin, L., et al., The Mathematical Theory of Optimal Processes, Interscience Publishers, John Wiley and Sons, New York, 1962.

16. Jacobson, D. and Mayne, D., Differential Dynamic Programming, New York: Elservier, 1970.

17. Sage, A., Optimum Systems Control, New Jersey: Prentice-Hall, Inc., 1968.

18. Bryson, A., Desai, M., and Hoffman, W., "Energy-State Approximation in Performance Optimization of Supersonic Aircraft," Journal of Aircraft, Vol. 6, No. 6, November-December, 1969, pp.481-488.

19. Calise, A., "Extended Energy Management Methods for Flight Performance Optimization," AIAA Journal, Vol. 15, No. 3, March 1977, pp.314-321.

20. Uehara, S., Stewart, H., and Wood, L., "Minimum-Time Loop Maneuvers of Jet Aircraft," Journal of Aircraft, Vol. 15, No. 8, August 1978, pp.449-455.

21. Calise, A., "Singular Perturbation Methods for Variational Aircraft Flight," IEEE Trans. Auto. Cont., Vol. AC-21, No. 3, June 1976, pp. 345-353.

22. Hedrick, J. and Bryson, A., "Three-dimensional Minimum-Time Turns for a Supersonic Aircraft," Journal of Aircraft, Vol. 9, pp. 115-121, February 1972.

23. Bryson, A. and Hedrick, J., "Three-dimensional Minimum-Fuel Turns for a Supersonic Aircraft," Journal of Aircraft, Vol. 9, pp.223-229, March 1972.

24. Hedrick, J. and Bryson, A., "Minimum-Time Turns for a Supersonic Airplane at Constant Altitude," J. Aircraft, Vol. 14, No. 8, August 1977, pp.182-187.

25. Erzberger, H. and Lee, H., "Optimum Horizontal Guidance Techniques for Aircraft," J. Aircraft, Vol. 8, No. 2, February 1971, pp.95-101.

26. Karmarkar, J., "Automated RNAV/MLS Transition -- An Avionics Sensitivity Study, Vol. III," NASA-CR-145109, March 1977.

27. Lee, H., McClean, J., and Erzberger, H., "Guidance and Control Techniques for Automated Air Traffic Control," J. Aircraft, Vol. 9, No. 7, July 1972, pp.490-496.

28. Marsh, J. and Grossberg, M., "Research Report for the Advanced Weapons Management System (AWMS)," Systems Control, Inc. Report to the Navy, Pacific Missile Test Center under Contract N00123-77-C-0633, June 1978.

29. Shultz, R. and Kilpatrick, P., "Aircraft Optimum Flight Paths," JANAIR Report 700709, June 1970.

30. Erzberger, H. and Lee, H., "Characteristics of Constrained Optimum Trajectories with Specified Range," NASA TM 78519, September 1978.

31. Funk, J., "Optimal-Path Precison Terrain-Following System," J. Aircraft, Vol. 14, No. 2, February 1977, pp.128-134.

32. Funk, J. and Breza, M., "An Integrated System for Thrust and Path Control During Terrain Following," to be published.

33. Trankle, T. and Bryson, A., "Autopilot Logic for the Flare Maneuver of STOL Aircraft," Stanford University SUDAAR Report No. 494, May 1975.

☆U.S.Government Printing Office: 1979 — 657-002/431